comptes rendus palevol
2026 • 25 • 9

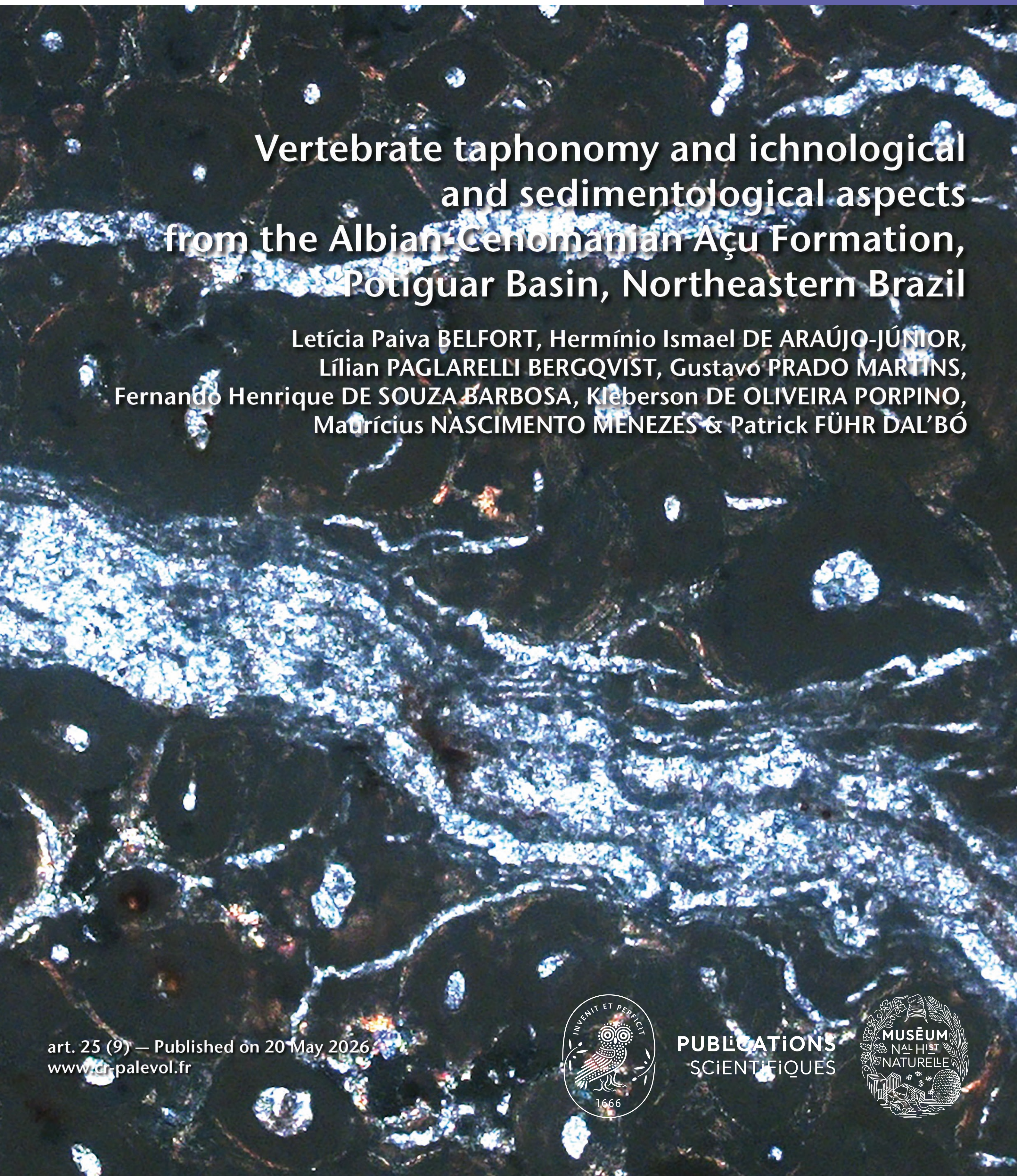

Vertebrate taphonomy and ichnological and sedimentological aspects from the Albian-Cenomanian Açu Formation, Potiguar Basin, Northeastern Brazil

Letícia Paiva BELFORT, Hermínio Ismael DE ARAÚJO-JÚNIOR, Lílian PAGLARELLI BERGQVIST, Gustavo PRADO MARTINS, Fernando Henrique DE SOUZA BARBOSA, Kleberson DE OLIVEIRA PORPINO, Maurícius NASCIMENTO MENEZES & Patrick FÜHR DAL'BÓ

art. 25 (9) — Published on 20 May 2026
www.cr-palevol.fr

PUBLICATIONS SCIENTIFIQUES
MUSÉUM NAL HIST NATURELLE

Couverture / *Cover*:
Diagenetic features in petrographic thin sections of specimens from collecting Site 2.3. Credits: Letícia Paiva Belfort, 2024.

Comptes Rendus Palevol est indexé dans / Comptes Rendus Palevol *is indexed by:*
- Cambridge Scientific Abstracts
- Current Contents® Physical
- Chemical, and Earth Sciences®
- ISI Alerting Services®
- Geoabstracts, Geobase, Georef, Inspec, Pascal
- Science Citation Index®, Science Citation Index Expanded®
- Scopus®.

Les articles ainsi que les nouveautés nomenclaturales publiés dans *Comptes Rendus Palevol* sont référencés par /
Articles and nomenclatural novelties published in Comptes Rendus Palevol *are registered on:*
- ZooBank® (http://zoobank.org)

Comptes Rendus Palevol est une revue en flux continu publiée par les Publications scientifiques du Muséum, Paris et l'Académie des sciences, Paris
Comptes Rendus Palevol *is a fast track journal published by the Museum Science Press, Paris and the Académie des sciences, Paris*

Les Publications scientifiques du Muséum publient aussi / *The Museum Science Press also publish:*
Adansonia, ***Geodiversitas***, ***Zoosystema***, ***Anthropozoologica***, ***European Journal of Taxonomy***, ***Naturae***, ***Cryptogamie* sous-sections *Algologie***, ***Bryologie***, ***Mycologie.***

L'Académie des sciences publie aussi / *The Académie des sciences also publishes:*
Comptes Rendus Mathématique, Comptes Rendus Physique, Comptes Rendus Mécanique, Comptes Rendus Chimie, Comptes Rendus Géoscience, Comptes Rendus Biologies.

Diffusion – Publications scientifiques Muséum national d'Histoire naturelle
CP 41 – 57 rue Cuvier F-75231 Paris cedex 05 (France)
Tél.: 33 (0)1 40 79 48 05 / Fax: 33 (0)1 40 79 38 40
diff.pub@mnhn.fr / https://sciencepress.mnhn.fr

Académie des sciences, Institut de France, 23 quai de Conti, 75006 Paris.

ISSN (imprimé / *print*): 1631-0683/ ISSN (électronique / *electronic*): 1777-571X

Vertebrate taphonomy and ichnological and sedimentological aspects from the Albian-Cenomanian Açu Formation, Potiguar Basin, Northeastern Brazil

Letícia Paiva BELFORT
Hermínio Ismael DE ARAÚJO-JÚNIOR
Department of Stratigraphy and Paleontology, Rio de Janeiro State University,
Rua São Francisco Xavier, 524 – Maracanã, 20550-013, Rio de Janeiro, RJ (Brazil)
leticiapaivabelfort@hotmail.com (corresponding author)

Lílian PAGLARELLI BERGQVIST
Macrofossil Laboratory, Department of Geology, Institute of Geoscience,
Federal University of Rio de Janeiro, Avenida Athos da Silveira Ramos,
274, Cidade Universitária, 21941-970, Rio de Janeiro, RJ (Brazil)

Gustavo PRADO MARTINS
Department of Stratigraphy and Paleontology, Rio de Janeiro State University,
Rua São Francisco Xavier, 524 – Maracanã 20550-013, Rio de Janeiro, RJ (Brazil)

Fernando Henrique DE SOUZA BARBOSA
Superior Normal School, Amazonas State University, Avenida Djalma Batista, 2470,
Chapada, 69050-300, Manaus, AM (Brazil)

Kleberson DE OLIVEIRA PORPINO
Department of Biological Sciences, State University of Rio Grande do Norte,
Avenida Prof. Antônio Campos, s/n, Costa e Silva 59610-090, Mossoró, RN (Brazil)

Maurícius NASCIMENTO MENEZES
Patrick FÜHR DAL'BÓ
Department of Geology, Institute of Geoscience, Federal University of Rio de Janeiro,
Avenida Athos da Silveira Ramos, 274, Bloco G, Centro de Ciências Matemáticas
e da Natureza (CCMN), 21941-970, Rio de Janeiro, RJ (Brazil)

Submitted on 16 December 2024 | Accepted on 20 January 2025 | Published on 20 May 2026

urn:lsid:zoobank.org:pub:91E35C56-F697-491E-BBA4-C4E370BBA70B

Belfort L. P., de Araújo-Júnior H. I., Paglarelli Bergqvist L., Prado Martins G., de Souza Barbosa F. H., de Oliveira Porpino K., Nascimento Menezes M. & Führ Dal'Bó P. 2026. — Vertebrate taphonomy and ichnological and sedimentological aspects from the Albian-Cenomanian Açu Formation, Potiguar Basin, Northeastern Brazil. *Comptes Rendus Palevol* 25 (9): 155-172. https://doi.org/10.5852/cr-palevol2026v25a9

ABSTRACT

Since the 19th century, vertebrate fossils from the Açu Formation (Potiguar Basin, northeastern Brazil) have received limited taphonomic attention, despite recent discoveries of various gnathostomes, including chondrichtyans, actinopterygians, dipnoans, crocodyliforms and dinosaurs. This study presents the first integrated macro- and microscale taphonomic analysis of vertebrate assemblages from selected outcrops of the Açu Formation. A total of 134 disarticulated vertebrate specimens, mainly vertebrae and limb bones, were examined, focusing on articulation, fragmentation, weathering, abrasion, bioerosion, root marks, and diagenetic features such as mineral replacement, pore filling, and fracturing. The assemblages record variable degrees of subaerial exposure and episodic transport prior to burial, as indicated by moderate abrasion, the predominance of weathering stage 2, insect bioerosion, tooth marks, and root traces. Petrographic analyses reveal extensive carbonate and iron oxide replacement, osteon infilling, and desiccation-related microfracturing, reflecting fossilization under generally humid conditions punctuated by intervals of reduced precipitation. Integrated sedimentological and taphonomic evidence indicates that the studied deposits accumulated within an estuarine floodplain system, most consistent with the upper, fluvial-dominated sector of an estuary. The predominance of fine-grained facies with pedogenic features, interbedded sandstones, and heterolithic bedding reflects episodic sedimentation under fluctuating hydrological conditions. The fossil assemblages comprise autochthonous to parautochthonous remains, recording localized burial, limited reworking, and temporal mixing during Cretaceous depositional processes.

KEY WORDS
Taphonomy,
ichnology,
diagenesis,
estuary,
Cretaceous.

RÉSUMÉ

Taphonomie des vertébrés et aspects ichnologiques et sédimentologiques de la formation d'Açu (Albien-Cénomanien), bassin de Potiguar, nord-est du Brésil.

Depuis le XIXe siècle, les fossiles de vertébrés de la formation d'Açu (bassin de Potiguar, nord-est du Brésil) ont fait l'objet d'une attention taphonomique limitée, malgré les récentes découvertes de divers gnathostomes, notamment des chondrichthyens, actinoptérygiens, dipneustes, crocodyliformes et dinosaures. Cette étude présente la première analyse taphonomique intégrée à l'échelle macro et micro des assemblages de vertébrés provenant d'affleurements sélectionnés de la formation d'Açu. Au total, 134 spécimens de vertébrés désarticulés, principalement des vertèbres et des os des extrémités, ont été examinés, en mettant l'accent sur l'articulation, la fragmentation, l'altération, l'abrasion, la bioérosion, les marques de racines et les caractéristiques diagénétiques telles que le remplacement minéral, le remplissage des pores et la fracturation. Les assemblages témoignent de degrés variables d'exposition à l'air libre et de transports épisodiques avant leur enfouissement, comme l'indiquent une abrasion modérée, la prédominance du stade d'altération 2, la bioérosion par les insectes, les marques de dents et les traces de racines. Les analyses pétrographiques révèlent un remplacement étendu par des carbonates et des oxydes de fer, un comblement des ostéons et des microfractures liées à la dessiccation, reflétant une fossilisation dans des conditions généralement humides ponctuées d'intervalles de précipitations réduites. Les données sédimentologiques et taphonomiques combinées indiquent que les dépôts étudiés se sont accumulés au sein d'un système de plaine inondable estuarienne, ce qui correspond le mieux au secteur supérieur, à dominance fluviale, d'un estuaire. La prédominance de faciès à grains fins présentant des caractéristiques pédogéniques, de grès intercalés et de stratification hétérolithique témoigne d'une sédimentation épisodique dans des conditions hydrologiques fluctuantes. Les assemblages fossiles comprennent des restes autochtones à parautochtones, qui témoignent d'un enfouissement localisé, d'un remaniement limité et d'un mélange temporaire au cours des processus de sédimentation du Crétacé.

MOTS CLÉS
Taphonomie,
ichnologie,
diagenèse,
estuaire,
Crétacé.

INTRODUCTION

Taphonomy is pivotal in elucidating the processes that govern the preservation of organic remains, including shells, mineralized skeletons, and trace fossils in the sedimentary record, and the transformation of a biocoenosis into a taphocoenosis (Behrensmeyer 1978, 1991; Kidwell & Flessa 1996; Rogers *et al.* 2007; Fernández-Jalvo & Andrews 2016). Over the past two decades, taphonomic studies have clarified pre-burial conditions and depositional contexts of Brazilian fossiliferous units by analyzing taphonomic alterations such as weathering, fractures, tooth marks, abrasion and disarticulation to infer biological and physical processes prior to burial (e.g., Araújo-Júnior & Moura 2014; Araújo-Júnior *et al.* 2015; Faria *et al.* 2020; De Oliveira *et al.* 2024). Taphonomic classifications, such as Behrensmeyer's (1978) weathering stages, have been instrumental in quantifying fragmentation, abrasion and weathering in fossils (e.g., Carvalho 2004; Araújo-Júnior & Porpino 2011; Araújo-Júnior *et al.* 2013a, b; Araújo-Júnior 2016; Martins *et al.* 2018; Trifilio *et al.* 2022).

Recent studies of the palaeofauna recovered from the Açu Formation sandstones (Cretaceous, Potiguar Basin) have identified at least eight dinosaur taxa but with only one species described for the basin (Pereira 2018; Pereira *et al.* 2020a, b, 2024), eight chondrichthyan taxa including *Distobatus* Werner, 1989 (Hybodontiformes) and the osteichthyans *Bawitius* Grandstaff, Smith, Lamanna, Lacovara & Abdel-Ghani, 2012 (bichir), Lepisosteidae Cuvier, 1825 (Ginglymodi), *Vidalamiinae* Grande & Bemis, 1998, *Pycnodontiformes* Berg, 1937 (Euteleostei), *Mawsonia* cf. *lavocati* (Sarcopterygii), *Asiatoceratodus* cf. *tiguidiensis* (Dipnoi), and *Ceratodus* Agassiz, 1838 (Dipnoi) (Veiga *et al.* 2019; Brito *et al.* 2025), as well as a crocodyliform taxon (Ribeiro *et al.* 2022). Additionally, indeterminate testudine remains (Bogado *et al.* 2021) and dinosaur tracks (Leonardi & Carvalho 2021) have been documented. This assemblage shares similarities with the Alcântara Formation (São Luís Basin) and North Africa lithostratigraphic units, notably the Kem Kem beds (Veiga *et al.* 2019; Pereira *et al.* 2021, 2024). Despite these fascinating discoveries, the taphonomic and depositional history of this assemblage remains poorly understood.

In this study, we investigate the taphonomic and ichnological characteristics of fossil accumulations in outcrops of the Açu Formation. Our findings provide new insights into the preservation process in fluvial-estuarine environments. Additionally, we offer a detailed analysis of specific aspects of the taphonomic and palaeoecological context of the Potiguar Basin during the Aptian-Cenomanian interval.

MATERIAL AND METHODS

The analyzed material consists of 134 reptile fossil specimens recovered from three sites of the Açu Formation: Site 1.1 (n = 22) and Site 1.2 (n = 14) at Outcrop 1, and Site 2.3 (n = 98) at Outcrop 2. These specimens were collected by the team of the Laboratório de Macrofósseis of the Universidade Federal do Rio de Janeiro (UFRJ) during fieldwork conducted between 2015 and 2019.

Stratigraphic sections at each outcrop were described following standard sedimentological procedures (Tucker 2011). This involved measuring bed thickness, recording lithological features (e.g., grain size, texture, and sedimentary structures such as cross-lamination, plane-parallel lamination), and noting the presence of fossils, intraclasts, and other components. Bed colors were determined using the Munsell Soil Color Chart (Munsell 2009).

Most specimens, primarily vertebrae and long bones assigned to Dinosauria and Testudines, are housed in the Fossil Reptile Collection of the Departamento de Geologia (DEGEO), Instituto de Geociências (IGEO), UFRJ.

The following biostratinomic features were evaluated: articulation and fragmentation (Behrensmeyer 1991; Lyman 1994; Araújo-Júnior *et al.* 2013a), bone representativeness (Shipman 1981), hydraulic equivalence (Behrensmeyer 1975; Araújo-Júnior *et al.* 2013a), bone transportability (Frison & Todd 1986; Araújo-Júnior *et al.* 2012), breakage patterns (Shipman 1981), weathering (Behrensmeyer 1978), abrasion (Shipman 1981; Simões *et al.* 2010; Fernández-Jalvo & Andrews 2016), trampling marks (Fiorillo 1988; Lyman 1994; Britt *et al.* 2009), invertebrate bioerosion (Pirrone *et al.* 2014), root marks (Behrensmeyer 1991; Nascimento 2020), and color patterns (Munsell 1994, 2009; Araújo-Júnior *et al.* 2013a). Due to limited taxonomic data and poor specimen preservation, precise age determination and the minimum number of individuals (MNI) could not be established.

Bone transportability for dinosaur material was assessed using the Fluvial Transport Index (FTI) (Frison & Todd 1986), which is based on empirical observations of large mammal skeletal element disarticulation and transport in fluvial settings and is suitable for large vertebrates (Araújo-Júnior *et al.* 2012). FTI groups comprise: 1) Group I (FTI ≥ 75): sacrum, patella, astragalus, calcaneum, and vertebra; 2) Group II (50 < FTI < 75): rib, scapula, humerus, tibia, and metacarpal; and 3) Group III (FTI ≤ 50): atlas, mandible, pelvis, radio-ulna, and femur. Higher FTI values indicate greater transportability in water currents. For Chelonian material, the Voorhies Group distribution was employed, as it is more suitable for medium-sized animals (Voorhies 1969; Araújo-Júnior *et al.* 2012).

To investigate micro-preservation and fossilization processes, 12 thin sections from specimens across the three sites were prepared and analyzed at the Laboratório Geológico de Processamento de Amostras (LGPA) of the Faculdade de Geologia of the Universidade do Estado do Rio de Janeiro (FGEL/UERJ), using Zeiss Axio Imager A2 polarized light microscope. Multiple sections from a single specimen were designated as R (right), M (middle), and L (left). These thin sections are housed in the Paleontological Collection of FGEL/UERJ.

For the diagenetic analysis, we employed the General Histological Index (GHI) (Hedges & Millard 1995; Hollund *et al.* 2011), along with assessing the degree of permineralization (Cassab 2010), the degree of replacement (Cassab 2010), and the degree of fragmentation (Behrensmeyer & Chapman 1993).

GEOLOGIC BACKGROUND

Regional geology of the Potiguar Basin

The Potiguar Basin is located in the northeastern region of the Brazilian Equatorial Margin, specifically within the states of Rio Grande do Norte and Ceará (Fig. 1). Its estimated area ranges from 48 000 km² and 60 000 km², depending on the study. Angelim *et al.* (2006), provide a geological map at a 1:500,000 scale, delineating geological units based on conservative stratigraphic and lithological criteria derived from surface outcrop data and traditional mapping techniques. In contrast, Pessoa-Neto *et al.* (2007), conducted under Petróleo Brasileiro S.A. (Petrobrás) employed geophysical and subsurface data, including seismic surveys and borehole profiles, to estimate the basin subsurface extension, often exceeding surface-observable limits. In this study, the delimitation and superficial geological aspects of the Potiguar Basin will be referenced according to the work of Angelim *et al.* (2006).

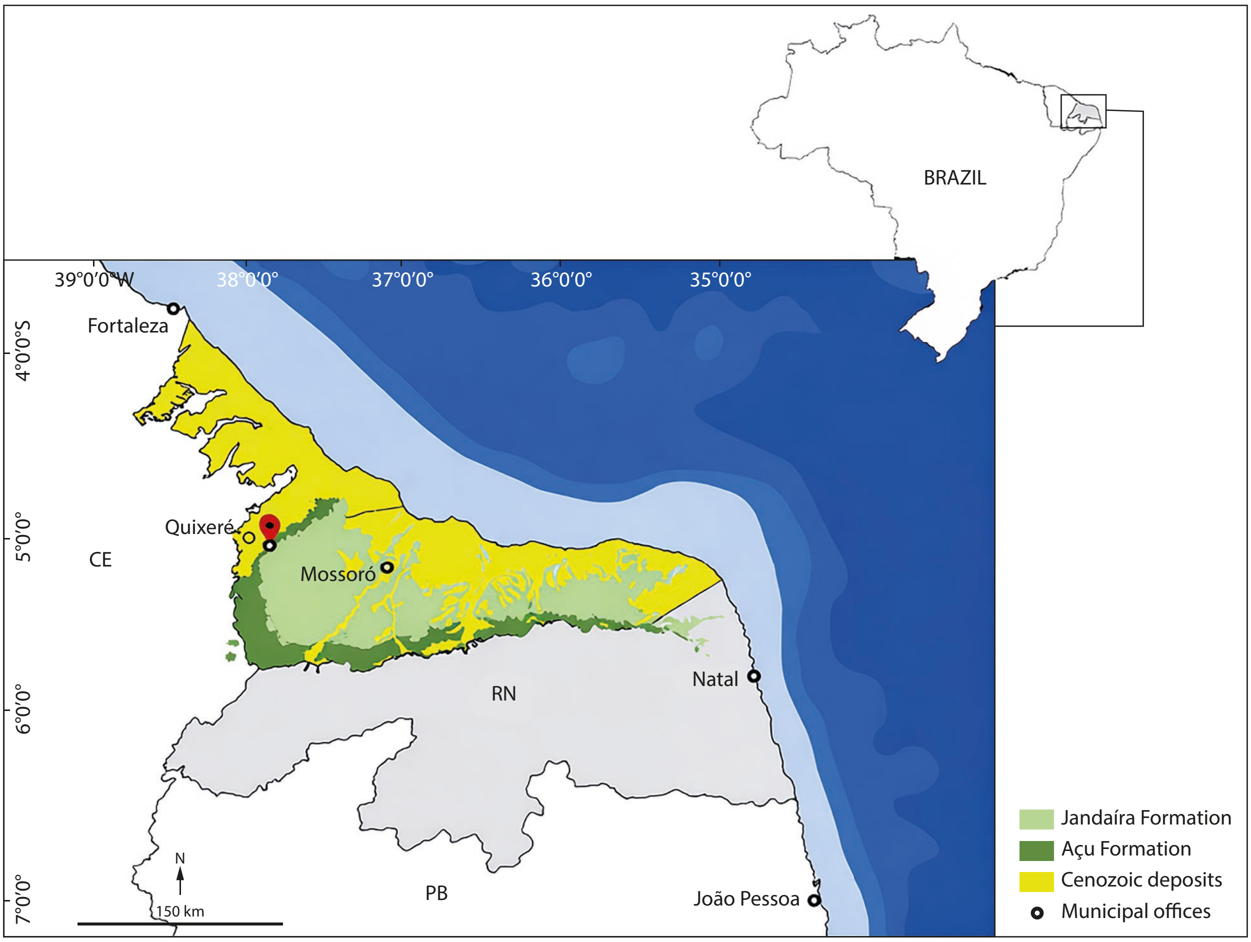

Fig. 1. — Simplified geological map showing the exposed portion of the Potiguar Basin. The **red pin** indicates the study area. Abbreviations: **CE**, Ceará; **PB**, Paraíba; **RN**, Rio Grande do Norte. Credits: Fernando Henrique de Souza Barbosa, 2024.

The Potiguar Basin originated during the Mesozoic period due to crustal stretching associated with the breakup of the Gondwana supercontinent (Matos 1992; Pessoa-Neto *et al.* 2007). This rifting occurred from the Late Jurassic to the Early Cretaceous period, leading to the separation of the African and South American plates and the formation of the South Atlantic Ocean (Angelim *et al.* 2006; Pessoa-Neto *et al.* 2007).

Araripe & Feijó (1994) proposed a lithostratigraphic framework for the basin, dividing its sedimentary succession into three groups in ascending stratigraphic order: Areia Branca, Apodi, and Agulha. The Apodi Group encompasses the Açu, Jandaíra, Ponta do Mel and Quebradas formations. The Açu Formation, the focus of this study, was first defined by Kreidler & Andery (1949), who describe it as composed of fine to coarse sandstones. Its dominant lithologies include thick beds of moderate to very thick sandstone, typically whitish, interbedded with shales, light green claystones, and reddish-brown siltstones, indicative of fluvial and estuarine depositional environments (Vasconcelos *et al.* 1990; Angelim *et al.* 2006).

Vasconcelos *et al.* (1990) divided the Açu Formation into four informal subunits (Açu 1 to Açu 4) based on electrical profiles from well data, which assess the rock electrical resistivity to infer composition, porosity, and fluid content. Only Açu 3 and Açu 4 subunits are exposed in outcrops. Açu 1 consists of conglomerate sandstones and ortho-conglomerates from braided fluvial systems. Açu 2 comprises coarse and conglomeratic sandstones transitioning to fine sandstones and siltstones, reflecting a shift from a braided to meandering river system. Açu 3 represents a high-energy alluvial-fluvial sequence, while Açu 4 includes coarse to fine sandstones, siltstones, shales, and carbonates deposited in tidal-dominated littoral-estuarine systems (Costa *et al.* 2014).

Initially dated as Turonian-Campanian (Upper Cretaceous) based on biostratigraphic analyses and stratigraphic correlations (Vasconcelos *et al.* 1990), the Açu 4 subunit was later revised to Albian-Cenomanian (Cretaceous) using palynological data (Araripe & Feijó 1994). More recent dinoflagellate studies suggest an Albian age (Arai 2009, 2014).

Study area

The study area encompasses two outcrops of the Açu 4 subunit, located in Quixeré municipality, Ceará state, Brazil. These outcrops are designated as "Outcrop 1" and "Outcrop 2". Three fossiliferous accumulations were identified and labeled as Site 1.1 (within Outcrop 1), Site 1.2 (within Outcrop 1), and Site 2.3 (within Outcrop 2), based on their specific locations (Fig. 2A).

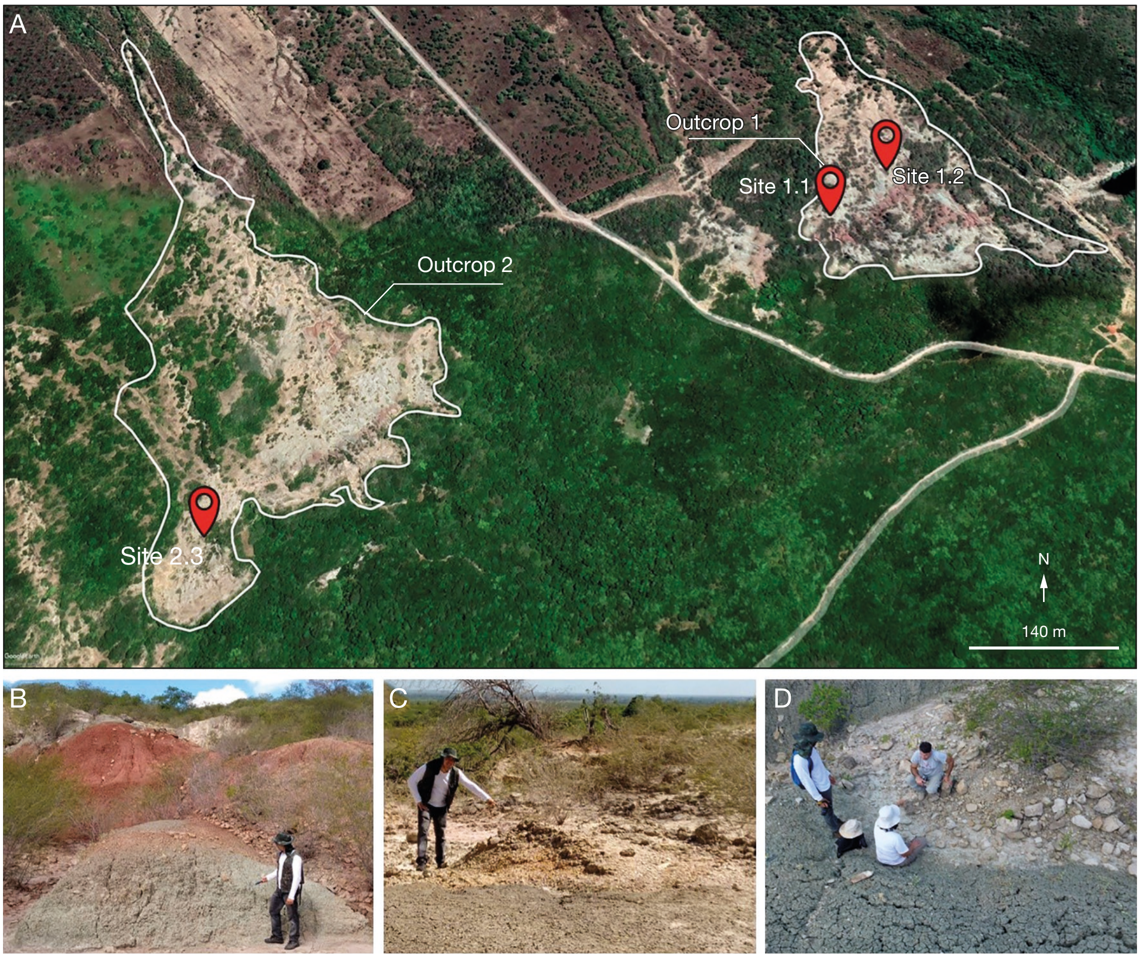

Fig. 2. — Aerial view of the two studied outcrops and collection sites discovered by the Macrofossil Laboratory/UFRJ team: **A**, location map of outcrops; **B**, Site 1.1; **C**, Site 1.2; **D**, Site 2.3. Credits: A, Letícia Paiva Belfort, 2024; B-D, Hermínio Ismael de Araújo Júnior, 2015.

Site 1.1

Site 1.1 exposes a short fluvial succession composed of three beds dominated by fine-grained deposits (Fig. 3A). The section is characterized by mudstones and very fine-grained sandstones exhibiting abundant pedogenic features, including slickensides, mottling, and carbonate concentrations, indicating recurrent subaerial exposure and soil-forming processes.

Plant remains occur on beds 1 and 3, whereas vertebrate fossils (semi-articulated sauropod long bones, including the diaphysis of appendicular element) are restricted to the uppermost bed. This fossiliferous horizon consists of mudstone lacking primary sedimentary structures and displaying well-developed pedogenic features, suggesting deposition in a low-energy, proximal environment subject to episodic sedimentation. The abrupt contact with the underlying sandstone, marked by carbonate nodules, indicates a discrete depositional event.

The stratigraphic organization of Site 1.1, combined with the restriction of vertebrate remains to a single bed, supports an interpretation of localized burial following subaerial exposure, consistent with floodplain deposition under fluctuating hydrological conditions.

Site 1.2

Site 1.2 is composed of a heterolithic fluvial succession dominated by alternating mudstones and fine- to very fine-grained sandstones, with frequent abrupt contacts between beds (Fig. 3B). The deposits display a predominance of greenish gray to light greenish gray colors, with common mottling, slickensides, and localized carbonate and iron concentrations, indicating recurrent pedogenic overprinting and episodic subaerial exposure.

Vertebrate remains are restricted to a single fossiliferous horizon (Bed 4), a heterolithic unit dominated by mudstone with interbedded fine sandstones and dispersed carbonized plant material. The occurrence of contraction structures within this bed suggests post-depositional clay deformation, consistent with repeated wet-dry cycles. Plant remains occur at several stratigraphic levels throughout the section, indicating sustained vegetal input in a low-energy depositional setting.

The stratigraphic architecture of Site 1.2, characterized by heterolithic facies, limited evidence of high-energy transport, and repeated indicators of subaerial exposure, is consistent with deposition in a proximal fluvial environment, likely a floodplain subject to episodic sedimentation and pedogenic

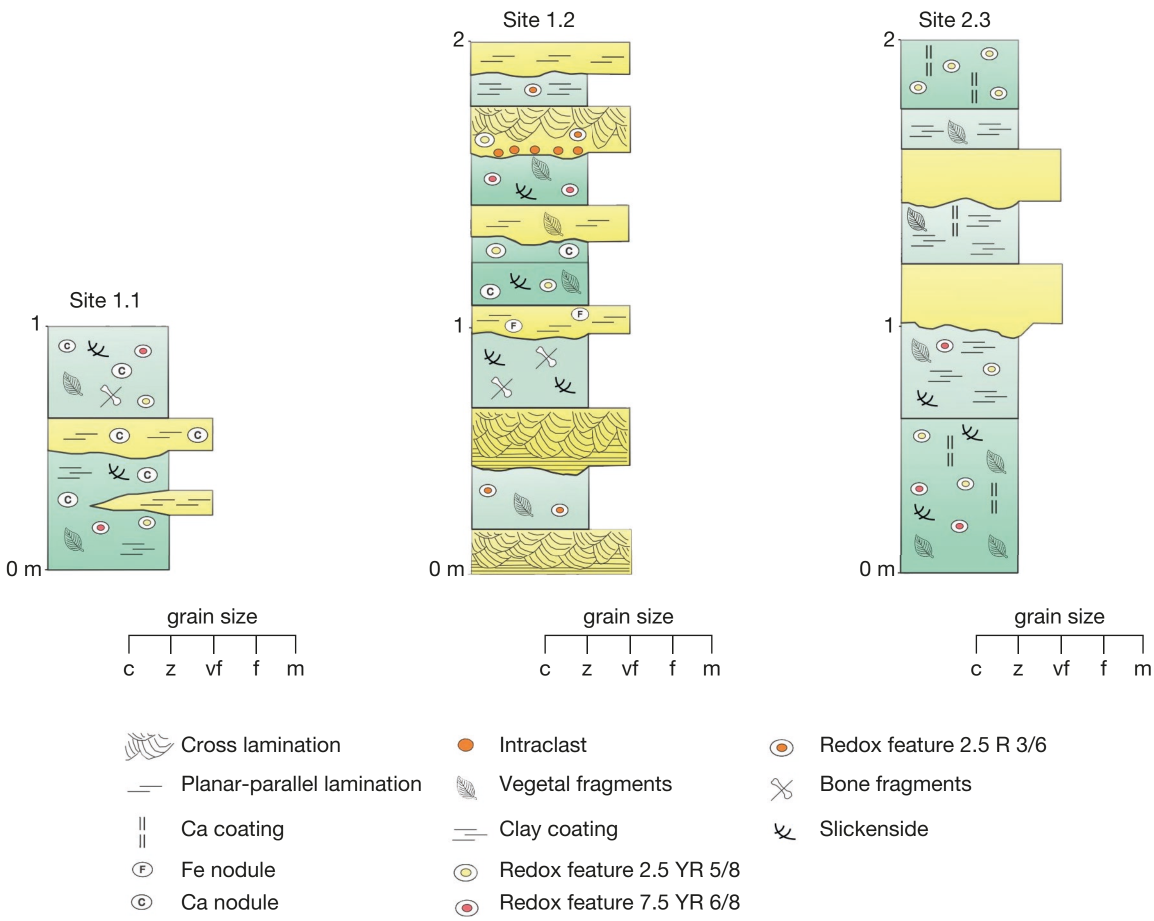

FIG. 3. — Stratigraphic profiles of the sites 1.1, 1.2 and 2.3 of the Açu Formation. The horizontal scale bar at the bottom of each profile represents grain size or lithology. Symbols include sedimentary structures such as cross lamination (**<**) and planar-parallel lamination (**—**), as well as features including calcium coating (**Ca coating**), iron nodules (**F in circle**) calcium nodules (**C in circle**), intraclasts (**filled orange circle**), plant fragments (**leaf symbol**), clay lamination (**stacked short horizontal lines**), redox features (**colored circles** indicating variable geochemical conditions: 2.5R 3/6, 2.5YR 5/8, 7.5YR 6/8), bone fragments (**crossed bones symbol**), and slickenside (**wavy line**), representing striated surfaces produced by shear movement. Abbreviations: **c**, clay; **f**, fine sandstone; **m**, medium sandstone; **vf**, very fine sandstone; **z**, silt (mudstone). Credits: Maurícius Nascimento Menezes, 2024.

modification. The restriction of vertebrate fossils to a single bed suggests localized burial events rather than continuous accumulation across the section.

Site 2.3

Site 2.3 exposes a heterolithic succession composed predominantly of mudstones interbedded with very fine-grained sandstones, forming a low-energy fluvial sequence (Fig. 3C). The deposits are characterized by abundant pedogenic and diagenetic features, including mottling, slickensides, salt concentrations, and carbonized plant remains, indicating recurrent subaerial exposure and post-depositional modification.

Vertebrate remains, mainly vertebrae, were recovered within the stratigraphic succession but could not be confidently assigned to a single bed due to limited exposure continuity and minor post-depositional displacement along the outcrop surface prior to collection. Nevertheless, the fossils are stratigraphically associated with the sedimentary succession of the Açu Formation and do not represent superficial or modern accumulations.

The vertical arrangement of fine-grained facies, together with the scarcity of primary sedimentary structures and the frequent occurrence of pedogenic features, suggests deposition in a floodplain setting subject to episodic sedimentation and fluctuating hydrological conditions. The stratigraphic complexity of Site 2.3 reflects dynamic depositional processes, with repeated phases of exposure, soil development, and burial.

RESULTS AND DISCUSSION

SITE 1.1

Biostratinomy

At Site 1.1, twenty-two fossil remains were analyzed. Among the specific specimens identified there is a sauropod dinosaur specimen (UFRJ-DG 624-R; Fig. 4B), composed of eight smaller, sub numbered pieces found in a semi-articulated association; a right abelisaurid femur (UFRJ-DG 588-R; Fig. 4A); an indeterminate dinosaur caudal vertebra (UFRJ-DG 730-R; Fig. 4C); a titanosaurian anterior caudal vertebra

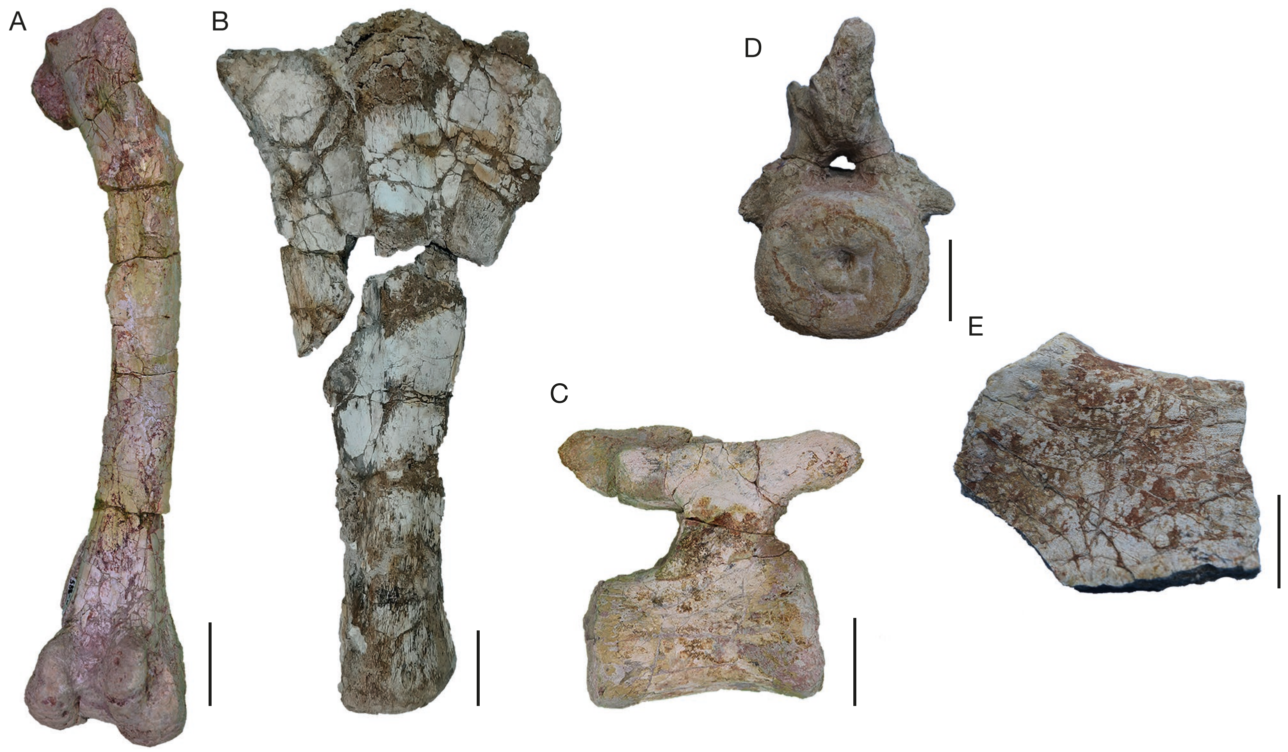

Fig. 4. — Diversity of vertebrate fossils from Site 1.1: **A**, semi-complete right femur assigned to Abelisauridae. UFRJ-DG 588-R, anterior view; **B**, semi-complete ulna attributed to a sauropod. UFRJ-DG 624-R, cranial view; **C**, sacral vertebrae of dinosaurs. UFRJ-DG 730-R, lateral view; **D**, sacral vertebra of Titanosauria (UFRJ-DG 674-R) in cranial view; **E**, a scapula (UFRJ-DG 731-R), lateral view, from Site 1.1. Scale bars: 5 cm. Credits: Letícia Paiva Belfort, 2024.

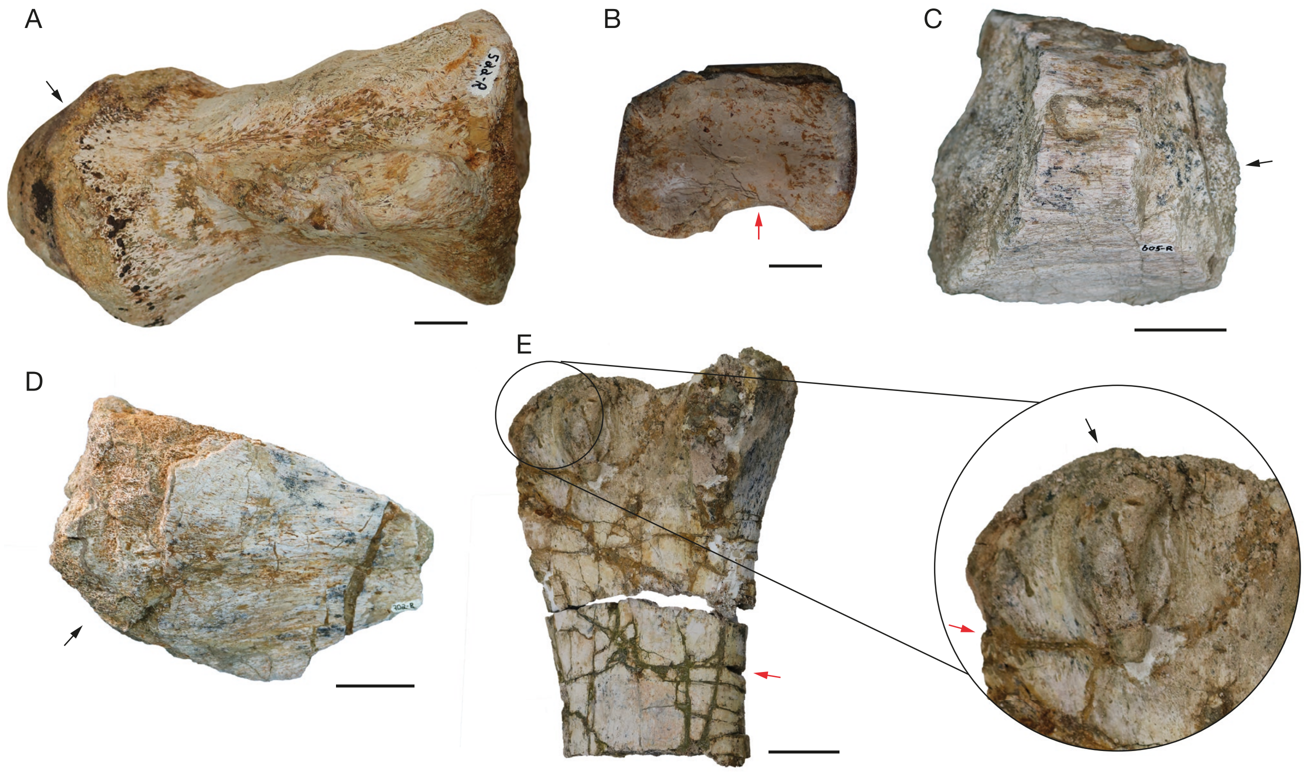

Fig. 5. — Stages of abrasion and weathering: **A**, caudal vertebral center of titanosauria, UFRJ-DG 522-R, side view, showing stage 3 of weathering; **B**, caudal vertebral od *Carcharadontosauria*, UFRJ DG-523-R, side view, showing stage 2 of weathering; **C**, fragment of Dinosauria, UFRJ-DG 605R with stage 3 of weathering and moderate level of abrasion; **D**, epiphysis of sauropod, UFRJ-DG 702-R with stage 4 of weathering and high level of abrasion; **E**, femur attirbuted to Sauropod, UFRJ-DG 624-R, dorsal view, with high level of abrasion. **Black arrows** indicate abrasion stages, and **red arrows** indicate weathering stages. Scale bars: 5 cm. Credits: Letícia Paiva Belfort, 2024.

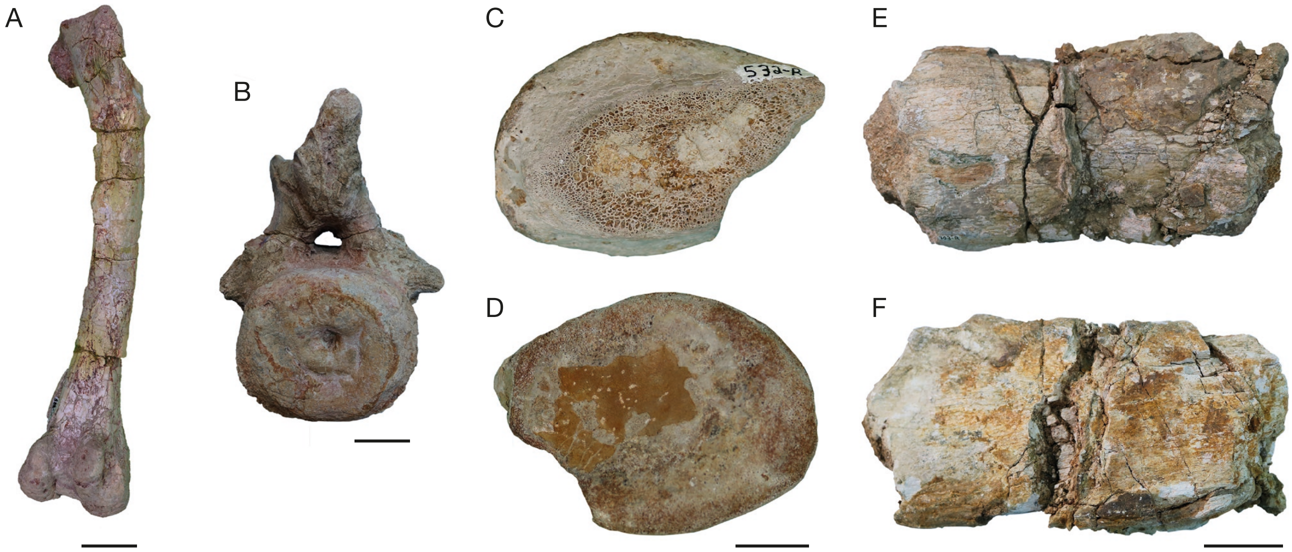

FIG. 6. — Taphonomic history of selected outcrops of the Açu 4 Unit: **A**, right femur of Abelisauridae (UFRJ-DG 588-R) in posterior view, with color pattern 5Y 8/4 gray yellow; **B**, sacral vertebra of Titanosauria (UFRJ-DG 674-R) in cranial view with color pattern 10YR 4/2 dark yellowish brown; **C**, **D**, UFRJ-DG 532-R, same fossil showing different colors: **C**, 5Y 8/4 grayish yellow; **D**, 10YR 5/4 moderate yellowish brown; **D**, Sauropod long bone diaphysis, UFRJ-DG 703-R, staining 10YR 7/4 gray orange on the dorsal portion and 5Y 7/6 moderate yellow on the ventral portion. Scale bars: 10 cm. Credits: Letícia Paiva Belfort, 2024.

(UFRJ-DG 674-R; Fig. 4D); and a scapula (UFRJ-DG 731-R; Fig. 4E). Of these, only the right abelisaurid femur and the sauropod specimen are nearly complete, while the others consist of fragmented remains.

Bone representation at Site 1.1 includes long bones and vertebrae of varying shapes, weight, and size (Fig. 5), suggesting that a hydraulic process contributed to the assemblage's formation.

At Site 1.1, the fossil remains exhibited different stages of weathering and abrasion, providing insights into their pre-burial histories. We identified weathering stages 1, 2, and 4. Weathering stage 1 was observed on the femur (UFRJ-DG 588-R), which also displayed slight abrasion. Specimens UFRJ-DG 674-R, UFRJ-DG 730-R, and UFRJ-DG 731-R presented Stage 2 of weathering and, similarly, also showed slight abrasion. In stark contrast, all eight specimens of the semi-articulated sauropod dinosaur (UFRJ-DG 624-R) were in Stage 4 of weathering and exhibiting heavy abrasion.

The variation in weathering stages suggests that the thanatocoenosis at Site 1.1 comprises material exposed for different periods before burial, with the semi-articulated sauropod being the most extensively exposed. Additionally, the distinct degrees of abrasion indicate different times and intensities of interaction between bones and sediment (Behrensmeyer & Miller 2012). Notably, the most heavily abraded specimens are precisely those with the most advanced stages of weathering, such as the semi-articulated sauropod.

Specimens from this site range in tones from 10YR to 5YR (greyish yellow and orange, dark yellowish brown, and pale greenish yellow; Munsell 1994). This variation is likely due to oxide impregnation (Fig. 7), which is associated with iron-rich soils characteristic of well-oxygenated environments (Fernández-Jalvo & Andrews 2016).

Vertebrate tooth marks were identified on the tibia of the semi-articulated sauropod (UFRJ-DG 624-R) and the distal portion of the abelisaurid right femur (UFRJ-DG 588; Fig. 8A). Additionally, root marks observed on an undetermined scapula (UFRJ-DG 731-R) (Fig. 8B) suggest that burial occurred in a humid, vegetated fluvial setting.

Analysis of the FTI at Site 1.1 revealed the presence of all three groups, with predominance of Group II (67%) (Fig. 5), which represents the category of material with the highest potential for transport due to attributes such as particle size, density, or shape. However, the absence of gravel and the dominance of sandstone with intercalations of silt and shale, indicate a low-energy depositional environment. Given the presence of tooth and root marks, which indicate minimal transport, along with the low-energy environment, the predominance of "more transportable" materials in FTI Group II does not suggest extensive transport. Rather, it implies that although these materials had the capacity for transport, the low-energy environment significantly constrained their actual displacement, resulting in relatively little transport of the fossil material.

Fossildiagenesis

Three thin sections (UERJ LM-006, UERJ LM-007, and UERJ LM-008) were prepared from highly fragmented, indeterminate specimens from Site 1.1 (Fig. 9). These highly fragmented fossils were selected due to their prolonged exposure to taphonomy processes.

The General Histological Index (GHI) ranges from 1 to 3, indicating small but well-preserved areas of Haversian channels and osteocytes lacunae (Hollund *et al.* 2011). The replacement rate is 80 to 90%. UERJ LM-006 exhibits predominantly dark iron oxide staining, with other colors present (Fig. 9A, B). UERJ LM-007 (Fig. 9C) and UERJ LM-008 (Fig. 9D-F) show a mix of carbonates and iron

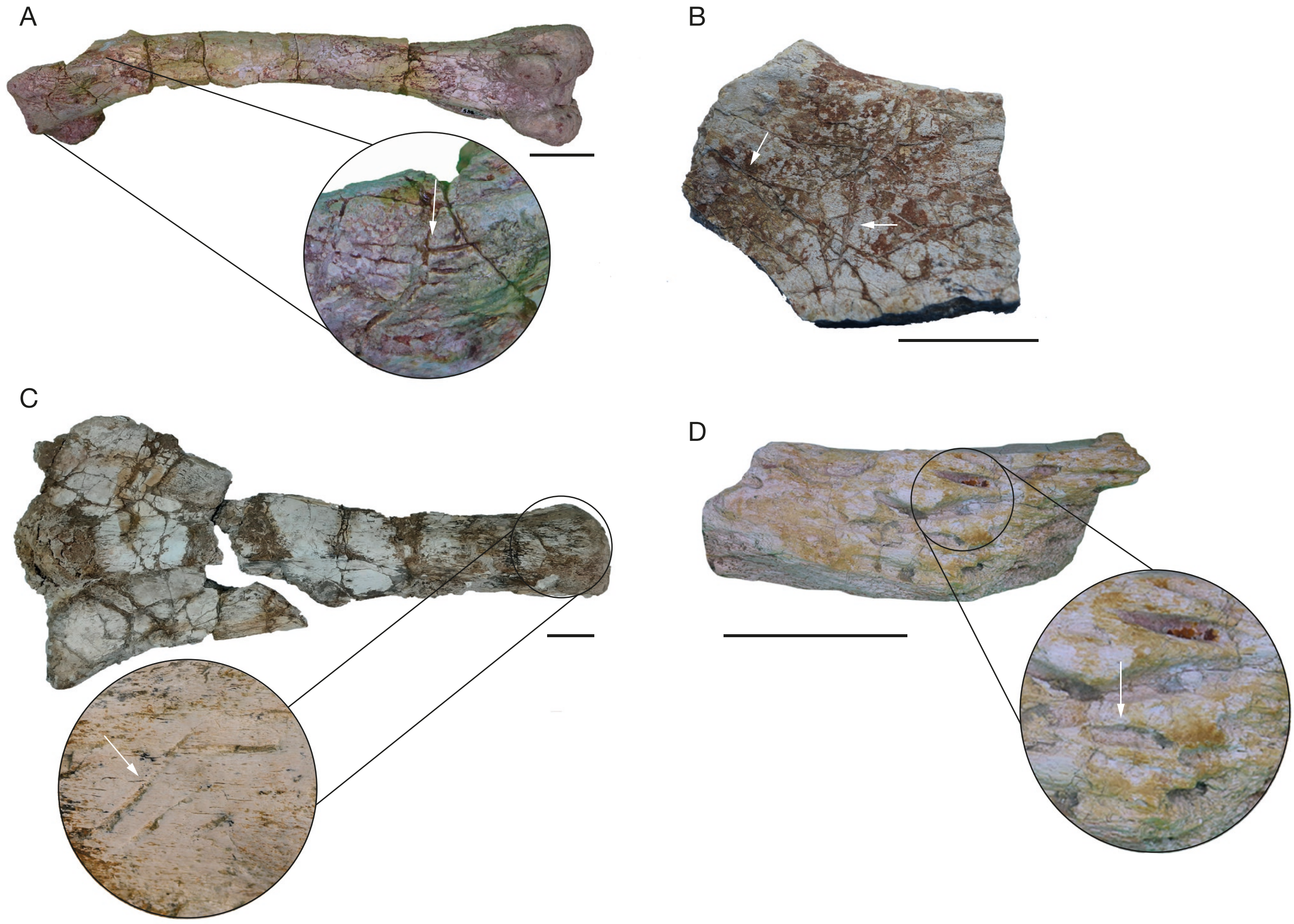

FIG. 7. — Biogenic marks observed on Dinosauria: **A**, UFRJ-DG 588-R with zoom indicating the location of tooth marks, site 1.1; **B**, fragment of a scapula, UFRJ-DG 731-R, site 1.1, showing root growth; **C**, anterior view of the possible tibia. UFRJ-DG 624-R with zooms, indicating the location of tooth marks, site 1.1; **D**, bioerosion traces attributed to the ichnogenus *Cubiculum* isp., UFRJ-DG 591-IC, site 2.3. Scale bars: A, C, D, 5 cm; B, 10 cm. Credits: A, Letícia Paiva Belfort, 2024; B-D, Hermínio Ismael de Araújo Júnior, 2018.

oxides. Permineralization also ranges from 80 to 90%, with large carbonate crystals, suggesting slow mineral growth over extended periods (Pfretzschner 2004). Iron oxide traces occur near osteon walls (UERJ LM-008). Carbonate precipitation in previously empty spaces has likely resulted from water-based transport and deposition during drying events, such as evaporation or declining groundwater levels (Pfretzschner 2004; Pfretzschner & Tütken 2011).

The formation of microfractures in osteons can be influenced by environmental conditions, with specific fractures emerging during dry periods and others associated with the alternation between wet and dry conditions. In prolonged dry conditions, circumferential cracks that isolate the osteons are formed. These fissures radiate from the osteon boundaries but do not extend much beyond them (Fig. 9A; see Pfretzschner & Tütken 2011). Meanwhile, extensive microfractures, which either transect or circumvent osteons, are potentially linked to drying events and physical weathering (Pfretzschner *et al.* 2001; Tütken *et al.* 2004). These diagenetic features, including the alternating formation of iron oxides and carbonates, suggest a history of intercalated wet and dry periods, which can influence the present fracture network.

SITE 1.2

Biostratinomy

At Site 1.2, fourteen specimens were analyzed, primarily fragmented chelonian plates. Most (*c.* 64%) exhibit slight abrasion, indicating minimal sediment interaction (Behrensmeyer & Miller 2012). Three additional specimens (UFRJ-DG 605-R; UFRJ-DG 702-R; UFRJ-DG 703-R), attributed to a theropod dinosaur, are also fragmented with a low level of abrasion. The majority (73%) display stage 2 of weathering (Fig. 5C).

These findings suggest moderate weathering at Site 1.2, which is slightly more intense than observed at Site 1.1. This higher intensity of weathering and the prevalence of stage 2 of weathering for most of the fossils, along with a high degree of fragmentation, abrasion, and weathering in the Dinosauria specimens, indicate significant and more prolonged subaerial exposure compared to Site 1.1.

The prevalence of stage 2 of weathering indicates variability within brown (10YR 4/2) for 73% of the samples, with two additional hues present. Additionally, the observation that the section of specimens exposed for a more extended period displays a darker color than the buried portion suggests differences in exposure conditions and/or duration.

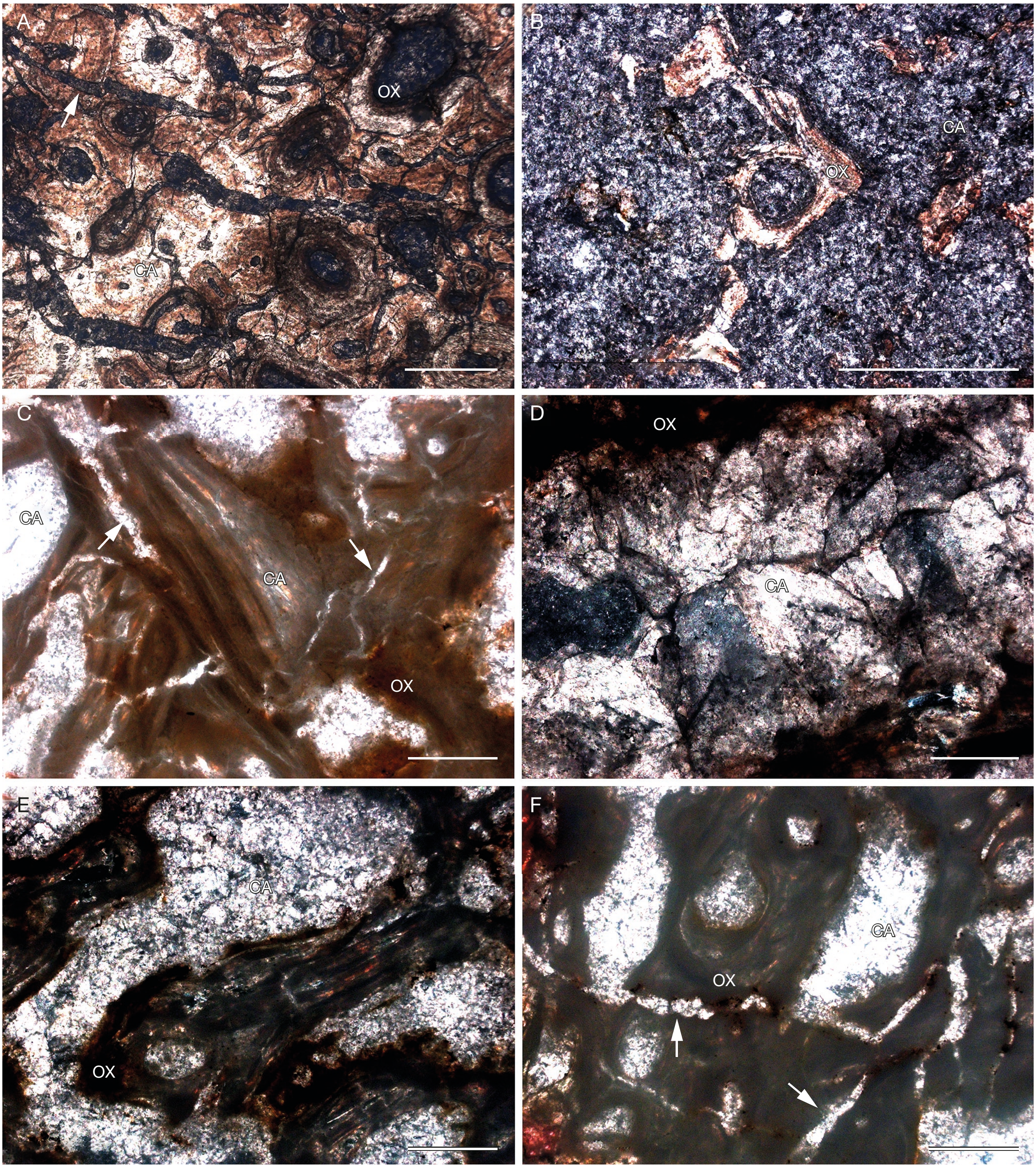

Fig. 8. — Diagenic features of Dinosauria in petrographic thin sections of specimens from collecting Site 1.1: **A**, UERJ LM-006, replacement by carbonate and iron oxide in the thin section. Photo under polarized light at 50x magnification; **B**, UERJ LM-006, replacement by iron oxide and filling with carbonate. Photo under polarized light at 50x magnification; **C**, UERJ LM-007, fractures (**white arrows**). Photo under natural light at 50x magnification; **D**, UERJ LM-008, filling with large carbonate crystals and replacement by iron oxide. Photo under polarized light at 100x magnification; **E**, UERJ LM-008 lade, replacement by iron oxide and filling by carbonate. Photo under polarized light at 50x magnification; **F**, UERJ LM-008, replacement by iron oxide, filling by carbonate and fractures (**white arrows**). Photo under polarized light at 50x magnification. Abbreviations: **CA**, carbonate; **OX**, iron oxide. Scale bars: A, C, E, F, 500 µm; B, 1000 µm; D, 200 µm. Credits: Letícia Paiva Belfort, 2024.

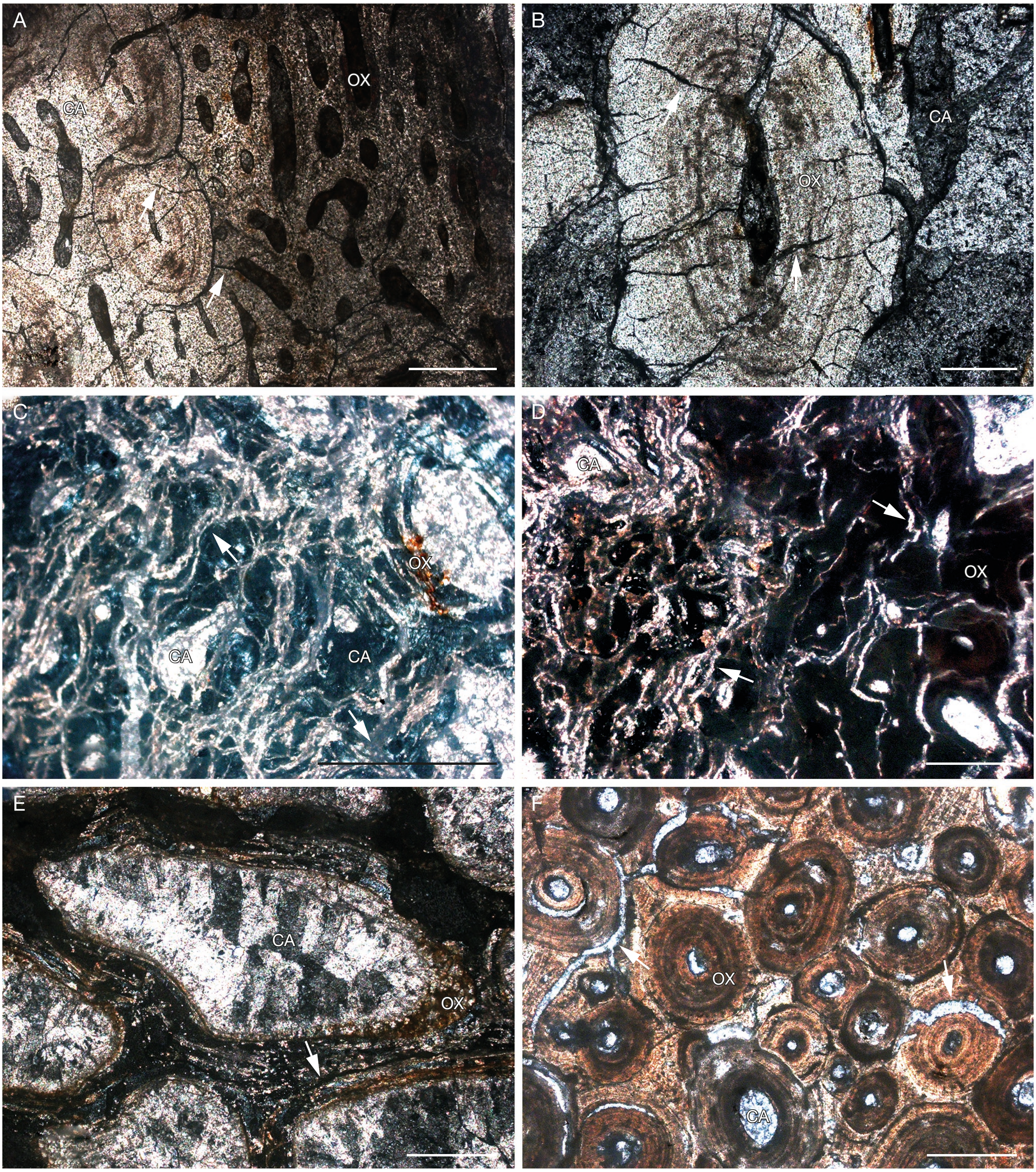

Fig. 9. — Diagenetic features in petrographic thin sections of specimens from collecting Site 1.2: **A**, UERJ LM-009, replacement by carbonate and iron oxide in the thin section; fracturing (**white arrows**). Photo under polarized light at 50x magnification; **B**, UERJ LM-009, iron oxide filling the concentric sheets and the Havers' canal filled with carbonate; fracture (**white arrows**). Photo under polarized light at 50x magnification; **C**, UERJ LM-010, fracturing (**white arrows**); different carbonate colors during replacement and filling; small presence of iron oxide. Photo under natural light at 50x magnification; **D**, UERJ LM-011, high fracture region with replacement by iron oxide and filling by carbonate. Photo under polarized light at 50x magnification; **E**, UERJ LM-012, replacement by iron oxide and filling by large carbonate crystals in Havers' canal, with fringes of carbonates. Photo under polarized light at 50x magnification; **F**, UERJ LM-013, replacement by iron oxide; filling by carbonate fractures (**white arrow**). Photo under polarized light at 100x magnification. Abbreviations: **CA**, carbonate; **OX**, iron oxide. Scale bars: A, D, E, 500 μm; B, 200 μm; C, 1000 μm; F, 20 μm. Credits: Letícia Paiva Belfort, 2024.

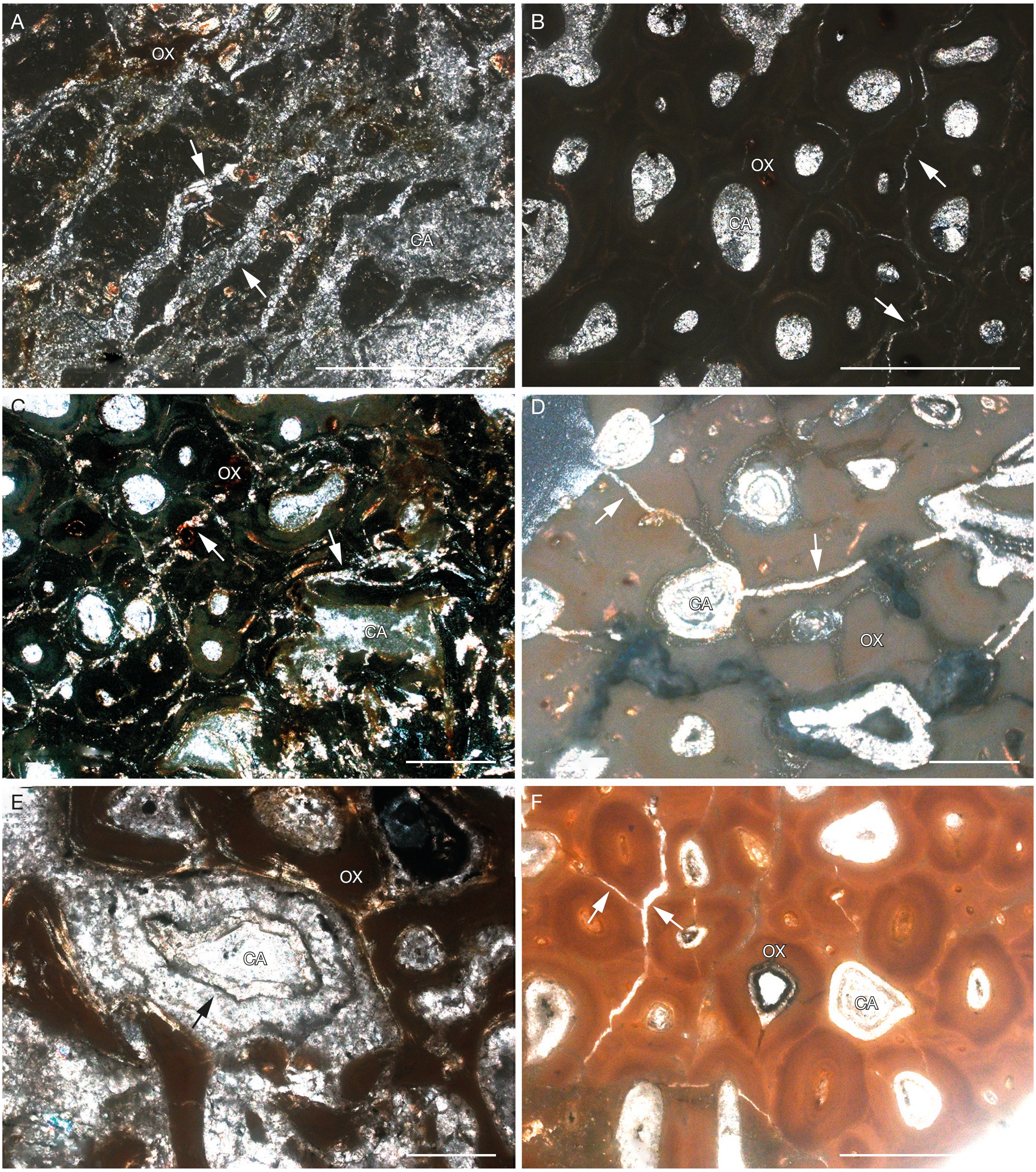

FIG. 10. — Diagenetic features in petrographic thin sections of specimens from collecting Site 2.3: **A**, UERJ LM-001, replacement by carbonate and iron oxide in the thin section, fractures (**white arrows**). Photo under polarized light at 50x magnification; **B**, UERJ LM-001, osteons replaced by iron oxide and filled with carbonate; fractures (**white arrows**). Photo under polarized light at 50x magnification; **C**, UERJ LM-002, fractures (**white arrows**); carbonate in the filling of Havers' canals and in the fractures; replacement by iron oxide. Photo under polarized light at 50x magnification; **D**, UERJ LM-003, bone tissue replaced by iron oxide, Havers' canals and fractures filled with carbonate, fracture (**white arrows**). Photo under polarized light at 50x magnification; **E**, UERJ LM-004, replacement by iron oxide and filling by large carbonate crystals in Havers' canal. Photo under polarized light at 50x magnification; **F**, UERJ LM-004, replacement by iron oxide; filling by carbonate; fractures (**white arrows**). Photo under polarized light at 100x magnification. Abbreviations: **CA**, carbonate; **OX**, iron oxide. Scale bars: A, B,1000 µm; C-E 500 µm; F, 20 µm. Credits: Letícia Paiva Belfort, 2024.

These variations in color and weathering stages (even not detailed for the remaining 27%) are indicative of temporal mixing (time averaging) within the Site 1.2 deposit, where materials with different exposure histories have been accumulated together.

Fossildiagenesis

Five thin sections (UERJ LM-009, UERJ LM-010, UERJ LM-011, UERJ LM-012 and UERJ LM-013) were produced from indeterminate fragmented specimens at Site 1.2 (Fig. 10), selected for their significant taphonomic features.

The GHI ranges from 0 to 1, indicating minimal preservation of the original bone tissue, with identifiable microstructures observable only in portions of UERJ LM-009 (Fig. 10A, B) and UERJ LM-013 (Fig. 10F). The degrees of replacement and filling degrees range between 80 and 90, with specimens exhibiting extensive replacement and filling by carbonate and iron oxide.

The histological sections reveal extensive fractures within and around the osteons, isolating them from surrounding structures, as well as carbonate fillings in the cracks, which point to prolonged drying of the bone (Pfretzschner & Tütken 2011). Additionally, some specimens display microfractures crossing several osteocytes, indicating physical weathering caused by decompression phenomena during uplift events (Behrensmeyer 1978; Previtera 2019).

Site 2.3

Biostratinomy

Ninety-eight specimens from Site 2.3, the most fossiliferous locality in the Açu Formation, were analyzed. Identified taxa include theropods (Maniraptora, Carcharodontosauria, Abelisauria and Megaraptora) and sauropods (Titanosauria and Rebbachisauridae) (Pereira *et al.* 2018, 2020a, b, 2024).

All analyzed specimens from Site 2.3 were recovered from buried contexts and are associated with defined stratigraphic levels within the Açu Formation. Although many remains were found disarticulated and fragmented, their occurrence within sedimentary beds indicates that the assemblage is stratigraphically controlled and not the result of recent surface accumulation or modern reworking. No taphonomic evidence indicative of prolonged recent exposure, such as fresh fractures, modern surface polishing, or differential weathering attributable to current climatic conditions, was observed. Therefore, the observed patterns of fragmentation, abrasion, and weathering are interpreted as the result of Cretaceous biostratinomic and early post-depositional processes rather than the product of recent erosional overprinting.

Of the recovered material, 51 vertebrae and one rib are partially complete, accompanied by 46 indeterminate fragments. Long bones exhibit breakage patterns B and D. All weathering stages are represented in the assemblage, with predominance of stages 2 (38%) and 3 (31%) suggesting a moderate subaerial exposure (Behrensmeyer 1978; Shipman 1981; Fernández-Jalvo & Andrews 2016). All four abrasion degrees are present, moderate abrasion being the most common pattern (41%), suggesting prolonged bone-sediment interaction (Behrensmeyer & Miller 2012; Fig. 5).

Insect traces identified as *Cubiculum* isp. (Roberts *et al.* 2007) were observed on eleven long bone fragments (Fig. 8D), measuring 1 to 3 cm in length and 0.5 cm in width (UFRJ-DG 591-ICV). These marks consist of ellipsoidal perforations in hollow, spongy cortical surfaces, with lengths being two to five times the diameter. The traces exhibit negative epirelief; high weathering obscures rounded bases and bioglyphs, precluding ichnospecific assignment. These traces, indicative of larval pupation (Roberts *et al.* 2007), represent the first record of this ichnospecies in the Açu Formation. Following Parkinson (2016), they are classified as type 2 chambers, characterized by: 1) maximum depth of 2 mm; 2) perpendicular orientation to the bone; 3) grouped or isolated arrangement; and 4) absence of padding or ramifications. The trace markers, probably beetles (Dermestidae), commonly known as skin beetles, are associated with a late stage of decomposition, targeting bones, cartilage, and skin (Huchet *et al.* 2013). Their presence suggests alternating humid and dry conditions, with seasonal moisture availability allowing insect activity during periods of carcass exposure, within an overall semi-arid climatic regime (Buatois & Mángano 2011; Pirrone *et al.* 2014). Fossil staining at Site 2.3 is relatively uniform in various shades of yellow 10Y, 10YR, and 5Y). Among specimens suitable for FTI analysis, Group I (highly transportable skeletal elements) predominates (45%). The presence of highly transportable elements, combined with moderate subaerial exposure and significant abrasion, indicates transport prior to final burial during Cretaceous depositional processes at Site 2.3.

Fossildiagenesis

Four thin sections (UERJ LM-001, UERJ LM-002, UERJ LM-003 and UERJ LM-004) were prepared from specimens of Site 2.3 (Fig. 10). While these fragments exhibit significant taphonomic features, they lack diagnostic morphological or structural characteristics (e.g., bone shape, bone growth patterns, or distinct cellular structures) necessary for taxonomic identification, rendering them taxonomically indeterminate.

These thin sections show a GHI of 0 (UERJ LM-001, Fig. 10A, B and UERJ LM-002, Fig. 10C) to 1 (UERJ LM-003, Fig. 10D and UERJ LM-004, Fig. 10E, F), indicating minimal preservation of the original tissue and significant loss of microstructural details. The substitution rate ranges from 80 to 90%, primarily involving iron oxide (which is evident through reddish to brownish staining). However, UERJ LM-001 (Fig. 10A, B) also demonstrates carbonate replacement. Extensive bone destruction in UERJ LM-001 (Fig. 10A, B) and UERJ LM-002 (Fig. 10C) indicates severe taphonomic alteration.

Permineralization ranging from 80 to 90%, suggests significant water availability during fossilization (Pfretzschner 2004; Trueman *et al.* 2004). Iron oxides are present in small areas, but carbonate infilling dominates, including carbonate fringes and mud within pores and fracture planes, likely resulting from cycling wet and dry events (Pfretzschner & Tütken 2011). Unlike Site 1.2, where infilling appears to be a single event, the concentric carbonate infilling in Haversian channels at Site 2.3 indicates multiple depositional episodes. Fracture patterns are similar to those at Site 1.2, with microfractures transecting or circumventing osteons.

Taphonomic history of selected outcrops of the Açu 4 Unit

The fossils from the three sites analyzed above exhibit similar taphonomic characteristics, suggesting comparable preservation processes, which are described below.

Site 1.1

The fossil assemblage at Site 1.1 exhibits clear evidence of temporal mixing, reflecting variable durations of subaerial exposure before burial. We identified diverse weathering stages (1, 2, and 4) in the fossils recovered from this site. This significant variation in weathering stages directly indicates that the thanatocoenosis at Site 1.1 comprises material that was exposed for different periods before burial. The semi-articulated sauropod, which is heavily abraded and presents Stage 4 of weathering, experienced the most extensive exposure (Araújo-Júnior & Marinho 2013). Fossil coloration, ranging from shades of yellow (5Y and 10Y) to brown (10YR), further supports this temporal heterogeneity, as this variation may also reflect differences in exposure time, environmental conditions, or sedimentation processes, suggesting that the deposit is not temporally homogeneous and contains fossils of different ages with distinct stages of preservation.

The presence of a semi-articulated sauropod skeleton suggests a relatively rapid burial after a period of subaerial exposure, indicating minimal or insignificant transport from the original death site (Behrensmeyer 1978), thus representing an autochthonous to parautochthonous accumulation (Araújo-Júnior 2016). The co-occurrence of isolated and disarticulated elements, along with slight to heavy abrasion, however, indicates some degree of short-distance transport (Behrensmeyer 1978; Badgley 1986; Araújo-Júnior *et al.* 2015). Although bite marks are present on some specimens, their low frequency suggests that direct predatory or scavenging activity played a secondary role in the taphonomic history of the assemblage. Fragmentation of remains is nevertheless common and is more consistently associated with prolonged subaerial exposure, transport, and post-depositional processes. The overall taphonomic signature of Site 1.1, characterized by varying degrees of weathering, abrasion, and coloration, reflects a dynamic depositional environment where organic remains underwent diverse post-mortem histories before final burial. The presence of both early and late weathering stages (1 and 4) suggests episodic depositional events rather than a single, rapid burial for the entire assemblage.

Site 1.2

The fragmented and lightly abraded specimens indicate minimal sediment interaction (Behrensmeyer & Miller 2012). The weathering stage of the majority of the specimens (stage 2) and the predominance of dark yellowish-brown coloration (10YR 4/2) suggest moderate weathering, slightly more intense than that observed at Site 1.1. This higher weathering intensity, combined with the prevalence of stage 2 and the high degree of fragmentation and abrasion observed in some specimens, indicates more prolonged subaerial exposure compared to Site 1.1, suggesting that fossils experienced different exposure durations or conditions.

Variations in color and weathering stages further indicate temporal mixing (time averaging) within the deposit at Site 1.2, where materials with distinct exposure histories were accumulated together. The fossil assemblage at Site 1.2, as in the other studied sites, does not exhibit abundant evidence of direct predatory activity, such as bite marks. The presence of low abrasion in some specimens suggests relatively rapid burial following subaerial exposure, indicating minimal or no transport from the original death site (Behrensmeyer 1978), consistent with a proximal depositional environment, possibly a floodplain setting. Thus, the assemblage represents an autochthonous to parautochthonous accumulation, similar to that observed at Site 1.1.

The taphonomic characteristics observed at Site 1.2, particularly moderate weathering, high fragmentation, evidence of time averaging, and limited transport, are comparable to those described for some fossil assemblages of the Romualdo Formation (Oliveira *et al.* 2011). These similarities suggest that both contexts were influenced by episodic exposure and burial in low-energy depositional environments, reinforcing the interpretation of dynamic depositional conditions with fluctuating hydrological regimes.

Site 2.3

Site 2.3 presents a fossil assemblage with a strong signature of prolonged subaerial exposure and significant temporal mixing. The assemblage included all weathering stages, with stages 2 (38%) and 3 (31%) being the most prevalent. This broad range of weathering, along with the generally disarticulated state of the fossils, indicates a prolonged period of exposure of the elements after death, prior to their final burial (Behrensmeyer 1991). The presence of multiple weathering stages within the assemblage highlights its temporal heterogeneity, indicating that fossils accumulated over different timeframes (e.g., Behrensmeyer 1990; Araújo-Júnior 2012).

Furthermore, the assemblage exhibits moderate abrasion, which, in conjunction with the presence of multiple weathering stages, indicates significant transportation to the depositional site (Behrensmeyer 1991). The notable portion of the assemblage that falls within the highly transportable FTI >75 group (Behrensmeyer 1990), reinforces that Site 2.3 represents a parautochthonous fossil accumulation, where remains were moved from their original death site but not necessarily over very long distances (Araújo-Júnior & Marinho 2013).

The presence of ichnofossils, specifically *Cubiculum* isp., is also crucial for understanding the taphonomic history. These traces, associated with dung beetle activity, suggest that the carcasses were exposed on a subaerial substrate for a sufficient period to allow insect colonization (Iniesto *et al.* 2021). The presence of fossilized dung beetle pupal chambers indicates a potentially seasonal environment with alternating dry and wet periods, allowing for both the desiccation of carcasses and subsequent burial episodes necessary for preservation (Pfretzschner 2004). This aligns with the varied weathering stages observed, as fluctuations in moisture could influence the rate and type of bone alteration (Pfretzschner & Tütken 2011). The diagenetic features observed at Site 2.3, such as concentric carbonate infilling in Haversian canals (as mentioned in the original Section 4.3.2), also indicate multiple depositional episodes, further supporting a complex post-mortem history for this site. The fossil assemblage at Site 2.3 is thus interpreted as a result of the selective accumulation of skeletal elements that underwent various degrees of decay, exposure, and transport.

Sedimentary environment interpretation

The Açu Formation has been interpreted as having been deposited in a fluvio-estuarine environment (Vasconcelos *et al.* 1990; Angelim *et al.* 2006; Veiga *et al.* 2023). An estuary is defined as the tide-influenced lower course of a river, where freshwater and seawater interact, forming a dynamic transition zone between terrestrial and marine environments. Simplistically, an estuary can be subdivided into three longitudinal sectors: a lower, marine-dominated reach; a central mixing zone; and an upper, fluvial-dominated reach. The estuarine floodplain comprises the low-lying, landward margin of the estuary, subject to periodic inundation by both river floods and high tides. This gently sloping area is dissected by a network of tidal creeks, natural levees, and backswamp depressions, forming a complex system of shallow channels that fill and drain twice daily with the tides, and more irregularly during river floods (Perillo 1995a, b). As water velocities decrease across this expansive surface, fine silts and clays, often enriched with organic matter, settle out, leading to the accumulation of thick, muddy floodplain deposits. These are occasionally interspersed with thin sand layers deposited by crevasse splays that breach levees during high-magnitude flood events (Koch *et al.* 2009; Perillo 2009).

Fossil accumulations are commonly associated with alluvial sedimentary environments. Although palaeontological research has traditionally focused on fluvial channel deposits, numerous studies have demonstrated that floodplain sediments also serve as significant repositories of fossil material (Bown & Kraus 1981; Behrensmeyer & Hook 1992; Behrensmeyer *et al.* 1995). Floodplains naturally attract animals seeking water, vegetation, or prey, making the floodplains frequent sites of mortality and subsequent accumulation of skeletal remains. The typically low-energy depositional environment of floodplains enhances the potential for fossil preservation.

Historically, vertebrate remains within fine-grained floodplain deposits are often interpreted as allochthonous, assumed to have been reworked from nearby fluvial channels during flood events or displaced across the floodplain by crevasse splay processes (Clark *et al.* 1967). However, increasing evidence suggests that these remains can also be autochthonous. They often display taphonomic signatures indicative of minimal transport, such as breakage, disarticulation, and sorting resulting from local in situ processes, including weathering, trampling, and winnowing (Behrensmeyer 1975; Bown & Kraus 1981).

Based on the detailed sedimentological descriptions and taphonomic analyses, the deposits examined from the Açu Formation, particularly at Sites 1.1, 1.2, and 2.3, are most consistent with the upper estuarine (fluvial-dominated) zone, precisely in the estuarine floodplain. The predominance of massive and laminated mudstones, exhibiting early pedogenic features such as slickensides and redoximorphic mottling, suggests prolonged subaerial exposure, pedogenesis, and low sedimentation rates, conditions typical of floodplain environments. Additionally, the occurrence of interbedded fine sandstones with plane-parallel or cross-laminations indicates episodic higher-energy depositional events. These may correspond to crevasse splays, minor distributary channels, or even weak tidal currents. The frequent presence of heterolithic bedding, thin alternations of sand and mud layers (1-5 mm thick), is indicative of tidal rhythmites or seasonal/episodic sedimentation, reflecting fluctuating flow energies. Furthermore, the association of these deposits with salt concentrations strengthens the interpretation of a mixed water regime, supporting a depositional setting influenced by both fluvial and tidal processes.

Palaeontological evidence further reinforces the interpretation of a floodplain environment. Taphonomic analyses reveal a mixed fossil assemblage, including both semi-articulated remains, indicative of minimal or no transport, and bones displaying moderate to high degrees of abrasion, suggestive of fluvial reworking and transport within channels, likely related to flooding events or crevasse splay activity. The presence of weathering marks across all assemblages, albeit at varying stages of modification, suggests that they underwent differential exposure durations before the final burial. Moreover, the high incidence of root traces, the presence of *Cubiculum* isp., and the abundance of phytoclasts reinforce the interpretation of a vegetated floodplain environment probably colonized by invertebrate organisms (although none have recovered so far). These features collectively indicate a dynamic setting where both autochthonous (in situ) and allochthonous (transported) fossil assemblages accumulated under fluctuating hydrological and ecological conditions typical of tidally influenced floodplain systems.

CONCLUSIONS

The fossil assemblages recovered from the three studied sites of Unit 4 of the Açu Formation record broadly comparable taphonomic histories, expressed with different intensities and degrees of temporal mixing. These assemblages reflect the combined effects of biostratinomic processes acting prior to burial and early fossildiagenetic modifications during shallow burial.

Biostratinomic signatures, including variable degrees of disarticulation, fragmentation, abrasion, weathering, bioerosion, and root marking, indicate differential durations of subaerial exposure prior to final burial. The coexistence of semi-articulated elements with isolated and highly fragmented remains suggests that skeletal materials experienced distinct post-mortem histories before incorporation into the sedimentary record.

The association of low to moderate energy sedimentary facies with predominantly limited transport supports the interpretation of autochthonous to parautochthonous fossil assemblages. Transport was episodic and localized, most likely related to flooding events and short-distance reworking within the depositional system, rather than sustained long-distance fluvial transport.

Microscale diagenetic features observed in thin sections, including extensive permineralization, carbonate and iron oxide replacement, osteon infilling, and desiccation-related microfracturing, indicate fossilization under generally humid conditions punctuated by intervals of reduced precipitation. These features are consistent with alternating wet and dry regimes operating during early diagenesis.

Integrated sedimentological and taphonomic data indicate that the studied deposits accumulated within an estuarine floodplain system, most consistent with the upper, fluvial-dominated sector of an estuary. The predominance of fine-grained deposits with pedogenic features, heterolithic bedding, and episodic sandy inputs reflects fluctuating hydrological conditions typical of tidally influenced floodplains. Together, these data indicate that the vertebrate assemblages of the Açu Formation formed through localized burial, limited reworking, and temporal mixing during Cretaceous depositional processes.

Acknowledgements

We are grateful to Coleção de Paleontologia of Universidade Federal do Rio de Janeiro (UFRJ) for allowing our access to the material analyzed. We also would like to thank the Laboratório Geológico de Processamento de Amostras of Universidade do Estado do Rio de Janeiro (LGPA/UERJ) for preparing the thin sections. We thank Ingrid Veiga (UERJ) for helping to edit the figures and Laís Alves-Silva for the support with graphics models. This work was supported by the Fundação de Amparo à Pesquisa do Estado do Rio de Janeiro [grant numbers: E-26/202. 829/2018 and E-26/203.176/2017] to LPB HIAJR, respectively. HIAJR also thanks to CNPq (grant no. 301405/2018-2). We also thanks the reviewers and the associate editor, Annalisa Ferretti.

REFERENCES

Angelim L. A. A., Nesi J. R., Torres H. H. F., Medeiros V. C., Santos C. A., Veiga Junior J. P. & Mendes V. A. 2006. — Geologia e Recursos Minerais do Estado do Rio Grande do Norte – Escala 1:500.000, *in* de Aquino A. L. A. (ed.), *Programa Geologia do Brasil*. CPRM – Serviço Geológico do Brasil, Recife, 119 p.

Arai M. 2009. — Paleogeografia do Atlântico Sul no Aptiano: um novo modelo a partir de dados micropaleontológicos recentes. *Boletim de Geociências da Petrobras* 17: 331-351.

Arai M. 2014. — Aptian/Albian (Early Cretaceous) paleogeography of the South Atlantic: a paleontological perspective. *Brazilian Journal of Geology* 44: 339-350.

Araripe P. T. & Feijó F. J. 1994. — Bacia Potiguar. *Boletim de Geociências da Petrobras* 8: 127-141.

Araújo-Júnior H. I. 2012. — *Tafonomia da acumulação fossilífera de vertebrados pleistocênicos do Tanque do Jirau, Itapipoca, Estado do Ceará, Brasil*. Dissertação (Mestrado em Geologia), Instituto de Geociências, Universidade Federal do Rio de Janeiro, Rio de Janeiro, 185 p.

Araújo-Júnior H. I. 2016. — Classifying vertebrate assemblages preserved in Quaternary tank deposits: implications for vertebrate taphonomy and paleoecology. *Palaeogeography, Palaeoclimatology, Palaeoecology* 445: 147-152. https://doi.org/10.1016/j.palaeo.2015.12.025

Araújo-Júnior H. I. & Marinho T. da S. 2013. — Taphonomy of a *Baurusuchus* (Crocodyliformes, Baurusuchidae) from the Adamantina Formation (Upper Cretaceous, Bauru Basin), Brazil: implications for preservational modes, time resolution and paleoecology. *Journal of South American Earth Sciences* 47: 90-99. https://doi.org/10.1016/j.jsames.2013.07.006

Araújo-Júnior H. I. & Moura G. J. B. 2014. — Anuros (Amphibia, Anura) do Pleistoceno Final–Holoceno inicial de Itapipoca, Estado do Ceará, Brasil: taxonomia, paleoecologia e tafonomia. *Revista Brasileira de Paleontologia* 17: 373-388. https://doi.org/10.4072/rbp.2014.3.08

Araújo-Júnior H. I. & Porpino K. O. 2011. — Assembleias fossilíferas de mamíferos do Quaternário do Estado do Rio Grande do Norte, Nordeste do Brasil: diversidade e aspectos tafonômicos e paleoecológicos. *Pesquisas em Geociências* 38 (1): 67-83.

Araújo-Júnior H. I., Bissaro-Júnior M. C., Santos T. T., Alves R. S. & Bergqvist L. P. 2012. — Tafonomia da megafauna pleistocênica brasileira: Fluvial Transport Index (FTI) em análises de representatividade óssea. *Revista Brasileira de Paleontologia* 15: 95-104.

Araújo-Júnior H. I., Porpino K. O., Ximenes C. L. & Bergqvist L. P. 2013a. — Unveiling the taphonomy of elusive natural tank deposits: a study case in the Pleistocene of northeastern Brazil. *Palaeogeography, Palaeoclimatology, Palaeoecology* 378: 52-74. https://doi.org/10.1016/j.palaeo.2013.04.001

Araújo-Júnior H. I., Porpino K. O. & Bergqvist L. P. 2013b. — Taphonomic analysis of a late Pleistocene vertebrate accumulation from Lage Grande paleontological site, Pernambuco state, northeastern Brazil: newremarks on preservational aspects of tank deposits. *Quaternary International* 317: 88-101. https://doi.org/10.1016/j.quaint.2013.08.016

Araújo-Júnior H. I., Porpino K. O. & Bergqvist L. P. 2015. — Vertebrate taphonomy and paleoecology in an Upper Pleistocene tank deposit of Paraíba, Brazil: taphonomic modes, evidence of temporal and spatial resolutions and paleoecological patterns of the Brazilian Intertropical Region. *Palaeogeography, Palaeoclimatology, Palaeoecology* 437: 1-17. https://doi.org/10.1016/j.palaeo.2015.07.009

Badgley C. 1986. — Counting individuals in mammalian fossil assemblages from fluvial environments. *Palaios* 1: 328-338. https://www.jstor.org/stable/3514695

Behrensmeyer A. K. 1975. — The taphonomy and paleoecology of Plio-Pleistocene vertebrate assemblage east of Lake Rudolf, Kenya. *Bulletin of the Museum of Comparative Zoology* 146: 473-578. https://www.biodiversitylibrary.org/page/4279538

Behrensmeyer A. K. 1978. — Taphonomic and ecologic information from bone weathering. *Paleobiology* 4 (2): 150-162. https://doi.org/10.1017/S0094837300005820

Behrensmeyer A. K. 1990. — Transport/hydrodynamics of bones, *in* Briggs D. E. G. & Crowther P. R. (eds), *Palaeobiology: A Synthesis*. Blackwell, Oxford: 232-235.

Behrensmeyer A. K. 1991. — Terrestrial vertebrate accumulations, *in* Allison P. A. & Briggs D. E. G. (eds), *Taphonomy: Releasing the Data Locked in the Fossil Record*. Plenum Press, New York, 291: 335.

Behrensmeyer A. K. & Chapman R. E. 1993. — Models and simulations of time-averaging in terrestrial vertebrate accumulations. *Short Courses in Paleontology* 6: 125-149. https://doi.org/10.1017/S2475263000001082

Behrensmeyer A. K. & Hook R. W. 1992. — Paleoenvironmental contexts and taphonomic modes, *in* Behrensmeyer A. K., Damuth J. D., Dimichele W. A., Potts R., Sues H. D. & Wing S. L. (eds), *Terrestrial Ecosystems Through Time: Evolutionary Paleoecology of Terrestrial Plants and Animals*. University of Chicago Press, Chicago: 15-136.
Behrensmeyer A. K. & Miller J. H. 2012. — Building links between Ecology and Paleontology using taphonomic studies of recent vertebrate communities, *in* Louys J. (ed.), *Paleontology in Ecology and Conservation*. Springer-Verlag, Berlin: 69-91. https://doi.org/10.1007/978-3-642-25038-5_5
Behrensmeyer A. K., Willis. B. J. & Quade J. 1995. — Floodplains and paleosols of Pakistan Neogene and Wyoming Paleogene deposits: implications for the taphonomy and paleoecology of faunas. *Palaeogeography, Palaeoclimatology, Palaeoecology* 15: 37-60.
Bogado J. P., Pereira L. G. C. P. V., Bergqvist L. P. & Fuente M. S. 2021. — *Turtles in a land of shrimp-eaters: fossil testudines of the potiguar basin*. Turtle Evolution Symposium 2021, Trelew: 67-67.
Bown T. M. & Kraus M. J. 1981. — Vertebrate fossil-bearing paleosol units (Willwood Formation, Lower Eocene, northwest Wyoming, U.S.A.): Implications for taphonomy, biostratigraphy, and assemblage analysis. *Palaeogeography, Palaeoclimatology, Palaeoecology* 34: 31-56. https://doi.org/10.1016/0031-0182(81)90057-2
Brito P. M., Veiga I. M., Dutheil D. B. & Bergqvist L. P. 2025. — First occurrence of *Distobatus* Werner, 1989 (Elasmobranchii: Hybodontiformes) in the middle Cretaceous (Albian-Cenomanian) of Brazil: taxonomic and biogeographical implications. *Cretaceous Research* 171 (106119): 1-7. https://doi.org/10.1016/j.cretres.2025.106119
Britt B. B., Eberth D. A., Scheetz R. D., Greenhalgh B. W. & Stadtman K. L. 2009. — Taphonomy of debris-flow dinosaur bonebeds at Dalton Wells, Utah (Lower Cretaceous, Cedar Mountain Formation, USA). *Palaeogeography, Palaeoclimatology, Palaeoecology* 280 (1-2): 1-22. https://doi.org/10.1016/j.palaeo.2009.06.004
Buatois L. A. & Mángano M. A. 2011. — *Ichnology: organism-substrate interactions in space and time*. Cambridge University Press, 347p.
Carvalho I. S. 2004. — *Paleontologia*. 2nd ed. Interciência, Rio de Janeiro, 258 p.
Cassab R. C. T. 2010. — Paleontologia: objetivos e princípios, *in* Carvalho I. S. (ed.), *Paleontologia: Conceitos e Métodos*. Interciência, Rio de Janeiro: 3-12.
Clark J., Beerbower J. R. & Kietzke K. K. 1967. — *Oligocene sedimentation, stratigraphy, paleoecology and paleoclimatology*. Geology memoirs, Fieldiana 5: 1-158.
Costa A. B. C., Córdoba V. C., Netto R. G. & Lima Filho F. P. 2014. — Registro faciológico e paleoambiental da transgressão que marca a passagem do Cenomaniano para o Turoniano na Bacia Potiguar, NE do Brasil. *Comunicações Geológicas* 101 Especial I: 415-420.
De Oliveira L. M., Araújo-Júnior H. I. D., Oliveira E. V. & Fambrini G. L. 2024. — Vertebrate taphonomy and taphofacies of the Capianga Member, Aliança Formation (Jurassic), Jatobá Basin, Brazil. *Journal of South American Earth Sciences* 147: 105122. https://doi.org/10.1016/j.jsames.2024.105122
Faria F. H. C., Carvalho I. S. & Araújo-Júnior H. I. 2020. — Genesis and taphonomic biases of Quaternary tank deposits of northeastern Brazil. *Quaternary International* 550: 184-193. https://doi.org/10.1016/j.quaint.2020.04.045
Fernández-Jalvo Y. & Andrews P. 2016. — Linear marks, *in* Delson E. & Sargis E. J. (eds), *Atlas of taphonomic identifications*. Springer, Dordrecht: 25-100. https://doi.org/10.1007/978-94-017-7432-1_3
Fiorillo A. R. 1988. — Taphonomy of Hazard Homestead Quarry (Ogallala Group), Hitchcock County, Nebraska. *Contributions to Geology* 26 (2): 57-97.
Frison G. C. & Todd L. C. 1986. — Taphonomic study of the Colby Site mammoth bones, *in* Frison G. C. (ed.), *The Colby Mammoth Site: Taphonomy and Archaeology of a Clovis Kill in Northern Wyoming*. University of New Mexico Press, Albuquerque: 24-90.
Hedges R. E. M. & Millard A. R. 1995. — Measurements and Relationships of Diagenetic Alteration of Bone from Three Archaeological Sites. *Journal of Archaeological Science* 22 (2): 201-209. https://doi.org/10.1006/jasc.1995.0022
Hollund H. I., Jans M. M, Collins E. M. J., Kars H., Joosten I. & Kars S. M. 2011. — What Happened Here? Bone Histology as a Tool in Decoding the Postmortem Histories of Archaeological Bone from Castricum, The Netherlands. *International Journal of Osteoarchaeology* 22 (5): 537-548. https://doi.org/10.1002/oa.1273
Huchet J. B., Le Mort F., Rabinovich R., Blau S., Coqueugiot H. & Arensburg B. 2013. — Identification of dermestid pupal chambers on Southern Levant human bones: inference for reconstruction of Middle Bronze Age mortuary practices. *Journal of Archaeological Science* 40 (10): 3793-3803. https://doi.org/10.1016/j.jas.2013.04.025
Iniesto M., Gutiérrez-Silva P., Dias J. J., Carvalho I. S., Buscalioni A. D. & López-Archilla A. I. 2021. — Soft tissue histology of insect larvae decayed in laboratory experiments using microbial mats: taphonomic comparison with Cretaceous fossil insects from the exceptionally preserved biota of Araripe, Brazil. *Palaeogeography, Palaeoclimatology, Palaeoecology* 564: 110156. https://doi.org/10.1016/j.palaeo.2020.110156
Kidwell S. M. & Flessa K. W. 1996. — The quality of the fossil record: populations, species, and communities. *Annual Review of Ecology and Systematics* 26: 269-299. https://www.jstor.org/stable/2097208
Koch E. W., Barbier E. D., Silliman B. R., Reed D. J., Perillo G. M. E., Hacker S. D., Granek E. F., Primavera J. H., Muthiga N., Polasky S., Halpern B. S., Kennedy C. J., Wolanski E., Kappel C. V., Aswani S., Cramer L. A., Bael D. & Stoms D. M. 2009. — Non-linearity in ecosystem services: temporal and spatial variability in coastal protection. *Frontiers in Ecology and the Environment* 7 (1): 29-37. https://doi.org/10.1890/080126
Leonardi G. & Carvalho I. S. 2021. — *Dinosaur Tracks from Brazil: A Lost World of Gondwana*. Indiana University Press, Bloomington, 468 p.
Lyman R. L. 1994. — *Vertebrate Taphonomy*. Cambridge University Press, Cambridge, 524 p. https://doi.org/10.1017/CBO9781139878302
Martins G. P. O., Santos A. C., Porpino K. O. & Araújo-Júnior H. I. 2018. — *Novas informações fossildiagenéticas sobre os vertebrados quaternários do tanque de Campo Alegre (Taperoá, Paraíba)*. XI Simpósio Brasileiro de Paleontologia de Vertebrados, Teresina, boletim de resumos, 63 p.
Matos R. M. D. 1992. — The Northeast Brazilian Rift System. *Tectonics* 11: 766-791.
Munsell A. H. 1994. — *Munsell soil color charts*. Revised edition. Macbeth Division of Kollmorgen Instruments Corporation, New Windsor, 29 p.
Munsell Color 2009. — *Geological rock-color chart with genuine Munsell color chips*. Munsell Color, Grand Rapids.
Nascimento D. L. 2020. — Rizólitos e Outros Traços Produzidos por Vegetais, *in* Sedorko D. & Francishini (eds), *Icnologia: Interações entre Organismos e Substratos*. CRV, Curitiba: 401-429.
Oliveira G. R., Saraiva A. A. F., Silva H. P., Andrade J. A. F. G. & Kellner A. W. A. 2011. — First turtle from the Ipubi Formation (Early Cretaceous), Santana Group, Araripe Basin, Brazil. *Revista Brasileira de Paleontologia* 14 (1): 61-66. https://doi.org/10.4072/rbp.2011.1.06
Parkinson A. H. 2016. — Traces of Insect Activity at Cooper's D Fossil Site (Cradle of Humankind, South Africa). *Ichnos* 23 (3-4): 322-339. https://doi.org/10.1080/10420940.2016.1202685

Pereira P. V. L. G. C. 2018. — *Fauna de dinossauros do Cretáceo (Albiano-Cenomaniano) da Formação Açu, Bacia Potiguar, Nordeste do Brasil*. Programa de Pós-graduação em Geologia, Universidade Federal do Rio de Janeiro, Tese de Doutorado, 126 p.

Pereira P. V. L. G. C., Marinho T. S., Candeiro C. R. A. & Bergqvist L. P. 2018. — A new titanosaur osteoderm record from Brazil and its significance. *Ameghiniana* 55 (6): 644-651. https://www.ameghiniana.org.ar/index.php/ameghiniana/article/view/3168

Pereira P. V. L. G. C., Ribeiro T. B., Brusatte S. L., Candeiro C. R. A., Marinho T. S. & Bergqvist L. P. 2020a. — Theropod (Dinosauria) diversity from the Açu Formation (mid-Cretaceous), Potiguar Basin, Northeast Brazil. *Cretaceous Research* 114: 104517. https://doi.org/10.1016/j.cretres.2020.104517

Pereira P. V. L. G. C., Veiga I. M. M. G, Ribeiro T. B., Cardozo R. H. B., Candeiro C. R. D. A. & Bergqvist L. P. 2020b. — The path of giants: a new occurrence of Rebbachisauridae (Dinosauria, Diplodocoidea) in the Açu formation, NE Brazil, and its paleobiogeographic implications. *Journal of South American Earth Sciences* 100: 102515. https://doi.org/10.1016/j.jsames.2020.102515

Pereira P. V. L. G. C., Bogado J. P., Ribeiro T. B., Belfort L. P., Valais S. & Candeiro C. R. A. 2021. — Dino on the menu: tooth traces in a sauropod epiphysis from the Presidente Prudente Formation (Campanian–Maastrichtian), Bauru Group, Brazil: palaeobiological and palaeoecological implications. *Historical Biology* 34 (11): 2079-2088. https://doi.org/10.1080/08912963.2021.2000603

Pereira P. V. L. G. C., Bandeira K. L. N., Vidal L. S., Ribeiro T. B., Candeiro C. R. A. & Bergqvist L. P. 2024. — A new sauropod species from north-western Brazil: biomechanics and the radiation of Titanosauria (Sauropoda: Somphospondyli). *Zoological Journal of the Linnean Society* 202 (4): zlae054. https://doi.org/10.1093/zoolinnean/zlae054

Pessoa-Neto O. C., Soares U. M., Fernandes da Silva J. G., Roesner E. H., Pires Florencio C. & Valentin de Souza C. A. 2007. — Bacia Potiguar. *Boletim de Geociências da Petrobras* 15 (2): 357-369.

Perillo G. M. E. 1995a. — Chapter 1. Geomorphology and sedimentology of estuaries: an introduction, *in* Perillo G. M. E. (ed.), *Developments in Sedimentology*. Vol. 53. Elsevier, Amsterdam: 1-16. https://doi.org/10.1016/S0070-4571(05)80021-4

Perillo G. M. E. 1995b. — Chapter 2. Definition and geomorphologic classifications of estuaries, *in* Perillo G. M. E. (ed.), *Developments in Sedimentology*. Vol. 53. Elsevier, Amsterdam: 17-47. https://doi.org/10.1016/S0070-4571(05)80022-6

Pfretzschner H. 2004. — Fossilization of Haversian bone in aquatic environments. *Comptes Rendus Palevol* 3 (6-7): 605-616. https://doi.org/10.1016/j.crpv.2004.07.006

Pfretzschner H.-U. & Tütken T. 2011. — Rolling bones: taphonomy of Jurassic dinosaur bones inferred from diagenetic microcracks and mineral infillings. *Palaeogeography, Palaeoclimatology, Palaeoecology* 310 (1-2): 117-123. https://doi.org/10.1016/j.palaeo.2011.01.026

Pfretzschner H.-U., Ashraf A. R., Maisch M. W., Sun G., Wang Y. & Mosbrugger V. 2001. — *Cyclic growth in dinosaur bones from the Upper Jurassic of NW China and its paleoclimatic implications*. Proceedings of the Sino-German Cooperation Symposium on Prehistory Life and Geology of Junggar Basin, Xinjiang, China, Urumqi: 21-39.

Pirrone C. A., Buatois L. A. & Riga B. G. 2014. — A new Ichnospecies of Cubiculum from Upper Cretaceous dinosaur bones in Western Argentina. *Ichnos: An International Journal for Plant and Animal Traces* 21 (4): 251-260. https://doi.org/10.1080/10420940.2014.958225

Previtera E. 2019. — Taphonomic analysis of saurischian dinosaurs from the Plottier Formation (Upper Cretaceous), Mendoza, Argentina. *Andean Geology* 46 (2): 345-367. https://doi.org/10.5027/andgeoV46n2-3161

Ribeiro T. B., Pereira P. V. L. G. C., Brusatte S. L., Candeiro C. R. A. & Bergqvist L. P. 2022. — An eye for an eye, a tooth for a tooth: archosaurian teeth from the Açu Formation (Albian–Cenomanian), Potiguar Basin, Northeast Brazil. *Cretaceous Research* 129: 105005. https://doi.org/10.1016/j.cretres.2021.105005

Roberts E. M., Rogers R. R. & Foreman B. Z. 2007. — Continental Insect Borings in Dinosaur Bone: examples from the late Cretaceous of Madagascar and Utah. *Journal of Paleontology* 81 (1): 201-208. https://www.jstor.org/stable/4133805

Rogers R. R., Eberth D. A. & Fiorillo A. R. 2007. — *Bonebeds: Genesis, Analysis and Paleobiological Significance*. University of Chicago Press, Chicago, 512 p.

Shipman P. 1981. — *Life History of a Fossil: An Introduction to Taphonomy and Paleoecology*. Harvard University Press, Cambridge, 222 p.

Simões M. G., Rodrigues S. C. & Bertoni-Machado C. 2010. — Procedimentos metodológicos em Tafonomia, *in* Carvalho I. S. (ed.), *Paleontologia: Conceitos e Métodos*. Interciência, Rio de Janeiro: 413-430.

Trifilio L. H. M. S., Araújo-Júnior H. I., Porpino K. O. & Barbosa F. H. S. 2022. — Mammal taphonomy in a cave deposit from Quaternary of Brazil. *Frontiers in Ecology and Evolution* 10: 830190. https://doi.org/10.3389/fevo.2022.830190

Trueman C. N. G., Behrensmeyer A. K., Tuross N. & Weiner S. 2004. — Mineralogical and compositional changes in bones exposed on soil surfaces in Amboseli National Park, Kenya: diagenetic mechanisms and the role of sediment pore fluids. *Journal of Archaeological Science* 31 (6): 721-739. https://doi.org/10.1016/j.jas.2003.11.003

Tucker M. E. 2011. — *Sedimentary Rocks in the Field: A Practical Guide*. 4th ed. Wiley-Blackwell, Chichester, 270 p.

Tütken T., Pfretzschner H.-U., Vennemann T. W., Sun G. & Wang Y. D. 2004. — Paleobiology and skeletochronology of Jurassic dinosaurs: implications from the histology and oxygen isotope compositions of bones. *Palaeogeography, Palaeoclimatology, Palaeoecology* 206 (3-4): 217-238. https://doi.org/10.1016/j.palaeo.2004.01.005

Vasconcelos E. P., Lima Neto F. F. & Roos S. 1990. — *Unidades de correlação da Formação Açu – Bacia Potiguar*. Congresso Brasileiro de Geologia, 36, Natal, SBG. Anais, v. 1: 227-240.

Veiga I. M. M. G., Berqgvist L. P. & Brito P. M. 2019. — The fish assemblage of the Cretaceous (?Albian-Cenomanian) Acu Formation, Potiguar Basin, Northeastern Brazil. *Journal of South American Earth Sciences* 93: 162-173. https://doi.org/10.1016/j.jsames.2019.04.015

Veiga I. M. M. G., Bergqvist L. P. & Brito P. M. 2023. — Paleoecological inferences on the fish assemblage of the Açu Formation (?Aptian–Cenomanian), Potiguar Basin, NE Brazil: a multiproxy approach. *Cretaceous Research* 142: 105411. https://doi.org/10.1016/j.cretres.2022.105411

Voorhies M. R. 1969. — Taphonomy and population dynamics of an early Pliocene vertebrate fauna, Knox County, Nebraska. *Contributions to Geology* 1: 1-69. https://doi.org/10.2113/gsrocky.8.special_paper_1.1

Submitted on 16 December 2024;
accepted on 20 January 2025;
published on 20 May 2026.